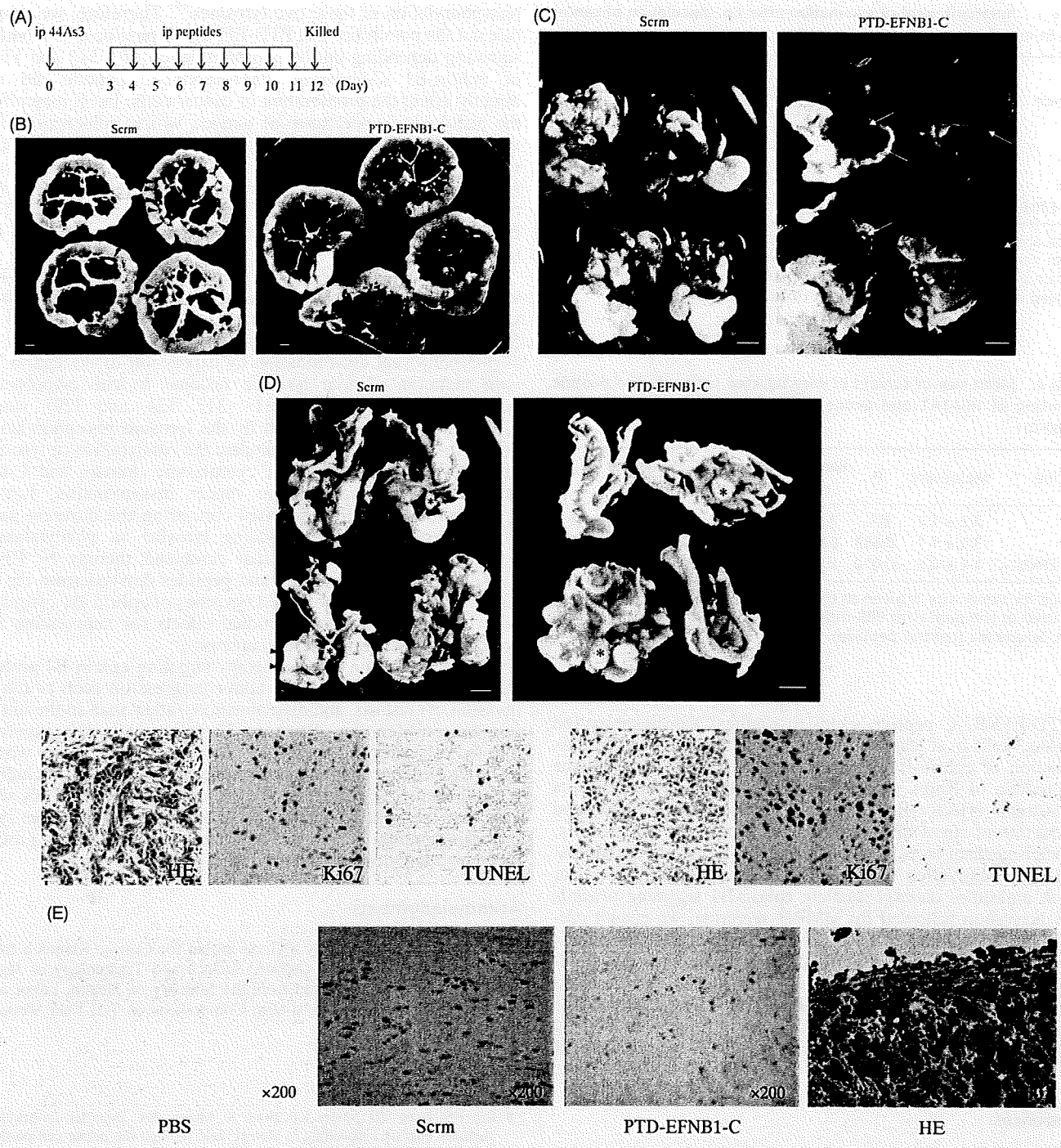

Fig. 4. Fusion protein PTD-EFNB1-C, consisting of the protein transduction domain of HIV-TAT and ephrin-B1$^{331-346}$, inhibits the peritoneal dissemination of scirrhous gastric cancer cells. (A) Time-course schedule of peritoneal dissemination assay. 44As3 scirrhous gastric cancer cells were transplanted in the peritoneal cavity of nude mice (ip). PBS containing control peptide Scrambled (Scrm) or PTD-EFNB1-C was intraperitoneally injected every 24 h after the transplantation of 44As3 cells. Representative appearance of intestinal loops (B) and the paragastric region (C), and tumors involving the rectouterine region (D) were compared. Red arrowheads (C,D) indicate disseminated tumor nodules. Yellow arrows (C) indicate fine tumor nodules in mesentery. In (D), all four mice treated with Scrm, but only one in four mice treated with PTD-EFNB1-C, show clear tumor dissemination. Asterisk indicates the bladder. No significant change was observed in the level of Ki67 and TUNEL staining. (E) Disseminated tumors of nude mice were subjected to immunostaining with anti-TAT antibody to detect the peptides in the tumor tissues. Histology of the tumor is shown at the bottom using H&E staining. PBS, mice treated with PBS without any peptide. Scale bars, 5 mm (B–D). Original magnification, ×200 (D bottom panels, E).

was widely distributed in the tumors *in vivo*, although not in all cells, indicates that the peptide was effectively incorporated into the tumor cells by intraperitoneal injection. It is expected that the tumor suppression effect of PTD-EFNB1-C will be further improved by modification of peptide delivery into tumors. The present study demonstrates the ability of a short peptide derived from the C-terminus of ephrin-B1 to suppress the invasion of cancer cells both *in vitro* and *in vivo*.

Table 1. Intraperitoneal dissemination after i.p. inoculation of cancer cells in mice†

Peptide	No. of nodules in mesentery‡			Paragastric region§	Rectouterine region§	No. of mice survived¶
	0–10	10–30	30+			
PBS	1	2	16	16	17	19
Scrm	1	3	14	16	16	18
PTD-EFNB1-C	12	4	3	3	3	19

†Data are shown as the number of mice bearing a tumor. ‡Number of tumor nodules larger than 2 mm in the mesentery per body. §Number of mice bearing tumor nodules larger than 5 mm. ¶Number of mice survived at 12 days after inoculation of cancer cells.

Table 2. Mean size of tumors in mice injected with a fusion peptide consisting of HIV-TAT and amino acids 331–346 of ephrin-B1 (PTD-EFNB1-C)†

Peptide	Mesentery	*P*	Paragastric region	*P*	Rectouterine region	*P*
PBS	3.2 ± 1.2	NA	7.5 ± 2.0	NA	8.0 ± 2.4	NA
Scrm	3.0 ± 1.1	0.683	6.8 ± 1.7	0.484	7.8 ± 2.1	0.532
PTD-EFNB1-C	1.4 ± 0.6	<0.010	1.8 ± 1.1	<0.001	2.3 ± 1.5	<0.001

†Value for tumor size is given as the mean ± SD (mm). Student's *t*-test was used to compare with PBS-treated group. NA, not applicable; Scrm, Scrambled (control peptide).

PTD-EFNB1-C peptide seems to suppress the dissemination of 44As3 cells in at least two ways. One is blocking the complex formation of ephrin-B1 with Dishevelled, which leads to the suppression of RhoA activation. Inactivation of RhoA and its downstream effector Rock likely suppresses the formation and contraction of stress fiber, thereby attenuating the cell motility. Another mechanism is blocking the MMP-8 secretion accompanied with inactivation of Arf1 GTPase. Because it is not clear which molecules directly mediate ephrin-B1 signaling towards Arf1 activation followed by MMP-8 secretion, we cannot currently conclude whether these two mechanisms are independent or whether they have some cross-talk. In addition, there is evidence that phosphorylation of two tyrosine residues located within the C-terminus of ephrin-B1 (Y343, Y344) affects the interaction with other proteins. For example, interaction of Dishevelled with ephrin-B1 is also regulated by the state of phosphorylation of these two tyrosines.[9] Therefore, we cannot rule out the possibility that PTD-EFNB1-C peptide also modifies signaling depending on the phosphorylation of Y343 and Y344 of ephrin-B1 C-terminus. PTD-EFNB1-C peptide did not directly affect the proliferation of cancer cells, but it may affect the histological appearance of tumors, which influences tumor volume (Fig. 4D). Stromal fibrosis is characteristic for gastric scirrhous carcinomas, and the proliferation of fibrous tissues may promote the growth and invasion of this type of tumor through some cancer–stromal interaction. Treatment of PTD-EFNB1-C peptide suppressed such stromal reaction within the tumors.

Besides the signaling related to the C-terminus of ephrin-B1, ephrin-B1 also induces the signaling through tyrosine phosphorylation of the cytoplasmic domain, which is mainly caused by Src family kinases. We previously reported the suppression of 44As3 peritoneal dissemination by expression of the ephrin-B1 with mutation of four tyrosine residues in the cytoplasmic domain (ephrin-B1 4YF; Y313, 317, 324, and 329), which blocks the signaling mediated by the tyrosine phosphorylation of ephrin-B1.[24] In order to compare the contribution of tyrosine phosphorylation of ephrin-B1 cytoplasmic domain and C-terminus mediated signaling to cancer dissemination, further systematic study will be required comparing the different parts of C-terminal peptides, including tyrosine to phenylalanine mutants. It is also possible that combined therapy by PTD-EFNB1-C used in this study and peptides derived from the aa surrounding the phosphorylated tyrosines of ephrin-B1 cytoplasmic domain might have additional effects for suppressing the promotion of scirrhous gastric carcinoma.

It appears that the peptide therapy targeting ephrin-B1 protein might have a major effect in tumor progression such as tumor invasion, metastasis, and dissemination, rather than in the initiation and proliferation of tumors. Therefore, it is also expected that the effects of the ephrin-B1 peptide on solid tumors would be improved by combination with other treatments including general chemotherapeutic reagents. Our results in this study suggest that the peptide derived from ephrin-B1 C-terminus is a promising model for novel drug design in scirrhous gastric carcinoma and possibly other types of tumors.

Acknowledgments

This work was supported by a Grant-in-Aid for Cancer Research from the Ministry of Education, Culture, Science and Technology of Japan and in part by a Grant-in-Aid from the Ministry of Health, Labor and Welfare of Japan for the third-term Comprehensive Ten-Year Strategy for Cancer Control.

References

1 Murai KK, Pasquale EB. Ephective signaling: forward, reverse and crosstalk. *J Cell Sci* 2003; **116**: 2823–32.
2 Blits-Huizinga C, Nelersa C, Malhotra A, Liebl D. Ephrins and their receptors: binding versus biology. *IUBMB Life* 2004; **56**: 257–65.
3 Poliakov A, Cotrina M, Wilkinson DG. Diverse roles of Eph receptors and ephrins in the regulation of cell migration and tissue assembly. *Dev Cell* 2004; **7**: 465–80.
4 Lin D, Gish GD, Songyang Z, Powson T. The carboxyl terminus of B class ephrins constitutes a PDZ domain binding motif. *J Biol Chem* 1999; **274**: 3726–33.
5 Cowan CA, Henkemeyer M. The SH2/SH3 adaptor Grb4 transduces B-ephrin reverse signals. *Nature* 2001; **413**: 174–9.
6 Bong YS, Park YH, Lee HS, Mood K, Ishimura A, Daar IO. Tyr-298 in ephrin-B1 is critical for an interaction with the Grb4 adaptor protein. *Biochem J* 2004; **377**: 499–507.
7 Tanaka M, Kamo T, Ota S, Sugimura H. Association of dishevelled with Eph tyrosine kinase receptor and ephrin mediates cell repulsion. *The EMBO J* 2003; **22**: 847–58.
8 Lee HS, Bong YS, Moore KB, Soria K, Moody SA, Daar IO. Dishevelled mediates ephrinB1 signalling in the eye field through the planar cell polarity pathway. *Nature Cell Biol* 2005; **8**: 55–63.
9 Lee HS, Mood K, Battu G, Ji YJ, Singh A, Daar IQ. FGF receptor-induced phosphorylation of ephrin-B1 modulates its interaction with Dishevelled. *Mol Boil Cell* 2009; **20**: 124–33.
10 Batlle E, Henderson JT, Beghtel H *et al.* Beta-catenin and TCF mediate cell positioning in the intestinal epithelium by controlling the expression of EphB/ephrinB. *Cell* 2002; **111**: 251–63.
11 Klein R. Eph/ephrin signaling in morphogenesis, neural development and plasticity. *Curr Opin Cell Biol* 2004; **16**: 580–9.
12 Batlle E, Bacani J, Begthel H *et al.* EphB receptor activity suppresses colorectal cancer progression. *Nature* 2005; **435**: 1126–30.
13 Tanaka M, Kamata R, Sakai R. Phosphorylation of ephrin-B1 via the interaction with claudin following cell-cell contact formation. *The EMBO J* 2005; **24**: 3700–11.
14 Holmberg J, Genander M, Halford MM *et al.* EphB receptors coordinate migration and proliferation in the intestinal stem cell niche. *Cell* 2006; **125**: 1151–263.

doi: 10.1111/j.1349-7006.2009.01352.x

15 Meyer S, Hafner C, Guba M *et al.* Ephrin-B2 overexpression enhances integrin-mediated ECM-attachment and migration of B16 melanoma cells. *Int J Oncol* 2005; 27: 1197–206.
16 Castellvi J, Garcia A, De la Torre J *et al.* EphrinB expression in epithelial ovarian neoplasms correlates with tumor differentiation and angiogenesis. *Hum Pathol* 2006; 37: 883–9.
17 Kataoka H, Tanaka M, Kanamori M *et al.* Expression profile of EFNB1, EFNB2, two ligands of EPHB2 in human gastric cancer. *J Cancer Res Clin Oncol* 2002; 128: 343–8.
18 Varelias A, Koblar SA, Cowled PA, Carter CD, Clayer M. Human osteosarcoma express specific ephrin profiles: implications for tumorigenicity and prognosis. *Cancer* 2002; 95: 862–9.
19 Tanaka M, Sasaki K, Kamata R, Sakai R. The C-terminus of ephrin-B1 regulates metalloproteinase secretion and invasion of cancer cells. *J Cell Sci* 2007; 120: 2179–89.
20 Siller-Lopez F, Garcia-Banuelos J, Hasty KA *et al.* Truncated active matrix metalloproteinase-8 gene expression in HepG2 cells is active against native type I collagen. *J Hepatol* 2000; 33: 758–63.
21 Stadlemann S, Pollheimer J, Moser PL *et al.* Cytokine-regulated expression of collagenase-2 (MMP-8) is involved in the progression of ovarian cancer. *Eur J Cancer* 2003; 39: 2499–505.
22 Lint PV, Libert C. Matrix metalloproteinase-8: cleavage can be decisive. *Cytokine Growth Factor Rev* 2006; 17: 217–23.
23 Futaki S, Suzuki T, Ohashi W *et al.* Arginine-rich peptides. *J Biol Chem* 2001; 276: 5836–40.
24 Tanaka M, Kamata R, Takigahira M, Yanagihara K, Sakai R. Phosphorylation of ephrin-B1 regulates dissemination of gastric scirrhous carcinoma. *Am J Pathol* 2007; 171: 68–78.
25 Tanaka M, Ohashi R, Nakamura R *et al.* Tiam1 mediates neurite outgrowth induced by ephrin-B1 and EphA2. *The EMBO J* 2004; 23: 1075–88.
26 Yanagihara K, Tanaka H, Takigahira M *et al.* Establishment of two cell lines from human gastric scirrhous carcinoma that possess the potential to metastasize spontaneously in nude mice. *Cancer Sci* 2004; 95: 575–82.

RET protein promotes non-adherent growth of NB-39-nu neuroblastoma cell line

Hitoyasu Futami and Ryuichi Sakai[1]

Growth Factor Division, National Cancer Center Research Institute, 5-1-1, Tsukiji, Chuo-ku, Tokyo 104-0044, Japan

(Received September 26, 2008/Revised January 30, 2009/Accepted February 11, 2009/Online publication March 23, 2009)

The receptor tyrosine kinase RET is expressed in a number of neuroblastoma tissues and cell lines, but its role in neuroblastoma remains to be determined. In this study, we examined the roles of RET protein in neuroblastoma by the RNA interference technique using the NB-39-nu neuroblastoma cell line. NB-39-nu neuroblastoma cells show high expression and elevated tyrosine phosphorylation of RET, although short interfering RNA against RET (RET siRNA) did not significantly inhibit cell proliferation or suppression of basal levels of phosphorylation of extracellular regulated kinase (ERK)1/2 or protein kinase B (AKT). By the addition of glial cell line-derived neurotrophic factor (GDNF), both the expression and phosphorylation of RET and the phosphorylation of ERK1/2 and AKT were further increased, whereas cell proliferation was not stimulated under normal culture conditions. However, proliferation of cells cultured under non-adherent conditions was significantly increased by GDNF. The increased proliferation was suppressed by RET siRNA, which also caused inhibition of the phosphorylation of ERK1/2 and AKT. These results suggest that RET signaling plays an important role in GDNF-induced enhancement of non-adherent proliferation of NB-39-nu cells, which might contribute to the metastasis of neuroblastoma. (*Cancer Sci* 2009; 100: 1034–1039)

RET is a receptor tyrosine kinase that is expressed in various neurons including central motor dopaminergic and noradrenergic neurons as well as peripheral enteric sensory and sympathetic neurons.[1,2] The expression of RET has also been detected in the mesonephric duct and branching ureteric bud during embryogenesis of the kidney.[1,2] It has been shown that RET is required for the development of the sympathetic, parasympathetic, and enteric nervous systems as well as the kidney and testis.[1,3] Dysfunctions of RET, which are caused by mutations of the gene, lead to various neuroendocrine tumors or enteric disorders. Germline gain-of-function mutations of RET are responsible for the dominantly inherited cancer syndromes of multiple endocrine neoplasia types 2A and 2B and familial medullary thyroid carcinoma.[4–6] In addition, somatic mutations or rearrangements of RET have also been found in sporadic medullary thyroid carcinoma and papillary thyroid carcinoma, respectively.[7–10] Loss-of-function mutations in RET have been found in some cases of Hirchsprung's disease characterized by severe constipation and intestinal obstructions during childhood.[11,12]

Neuroblastoma is the most common extracranial tumor in children and is derived from sympathoadrenal lineage of the neural crest in which RET is expressed.[13] Although RET is expressed in most neuroblastoma tissues and cell lines and its overexpression has been reported in some cell lines,[14–17] its role in molecular pathogenesis in neuroblastoma remains to be determined.

Glial cell line-derived neurotrophic factor (GDNF), a ligand of RET protein, was originally purified as a growth factor promoting survival of the embryonic dopaminergic neurons and exhibiting a potent trophic factor for spinal motor neurons and central noradrenergic neurons.[18–20] GDNF induces dimerization of RET in the form of multicomponents with a coreceptor GDNF family receptor α 1 (GFRα-1) and triggers autophosphorylation of RET in its intracellular tyrosine kinase domain. The phosphorylated tyrosines serve as docking sites for signaling molecules such as Shc, FRS2, IRS1/2 and Dok1/4/5.[21] In neuroblastoma, it has been shown that extracellular regulated kinase (ERK), phosphoinositide 3-kinase/protein kinase B (AKT), c-Jun N-terminal kinase, and p38 mitogen-activated protein kinase (p38MAPK) pathways are activated mainly through tyrosine 1062,[22] but their biological effects have not been fully elucidated.

In this study, we investigated the biological role of RET in neuroblastoma using the NB-39-nu neuroblastoma cell line, which shows extremely high expression and elevated phosphorylation of RET, by suppression of RET protein expression using RNA interference (RNAi).

Materials and Methods

Cell line and culture. NB-39-nu, Nagai,[23] and YT-nu[24] were provided by the Carcinogenesis Division, National Cancer Center Research Institute (Tokyo, Japan). NB-1 and TNB-1 were obtained from the Human Science Research Resource Bank (Tokyo, Japan). SK-N-SH was obtained from Riken Cell Bank (Tsukuba, Japan) and TT was obtained from the American Type Culture Collection (Manassas, VA, USA). These cell lines were maintained in RPMI-1640 medium with 10% heat-inactivated fetal bovine serum, 100 units/mL penicillin, and 100 μg/mL streptomycin at 37°C with 5% CO_2.

Short interfering RNA. Short interfering RNA against human RET (RET siRNA) was generated using a BLOCK-iT RNAi TOPO Transcription Kit and BLOCK-iT Complete Dicer RNAi Kit (Invitrogen, Carlsbad, CA, USA) according to the manufacturer's instructions. In the generation of RET siRNA, 805 bp from the second nucleotide of the initiation codon of human RET was chosen as the target sequence, and amplified by polymerase chain reaction using human RET cDNA and the primers, 5′- tggcgaaggcgacgtccggt-3′ and 5′-cgagtcgtcctcgtcgtaca-3′. The control LacZ siRNA was made using an expression plasmid containing the lacZ gene and polymerase chain reaction primers attached in the kit. Transfection was carried out with Lipofectamine 2000 (Invitrogen).

Antibodies and reagents. Anti-ERK1/2 antibody, anti-phospho-ERK1/2 antibody (phospho-p44/p42 mitogen-activated protein kinase antibody), anti-AKT antibody, and anti-phospho-AKT (Ser473) antibody were purchased from Cell Signaling Technology (Danvers, MA, USA). Anti-RET (C-19) antibody and Chr-A (chromogranin-A) were purchased from Santa Cruz Biotechnology (Santa Cruz, CA, USA). Anti-α-tubulin (B-5-1-2) antibodies were purchased from Sigma (St. Louis, MO, USA). Anti-GAP-43 was purchased from Zymed Laboratories (San Francisco, CA, USA). Anti-phospho-RET antibody was produced by immunizing rats with a synthetic phospho-peptide corresponding to residues around Tyr1062 of a long form of human RET. Horseradish peroxidase-conjugated anti-mouse and anti-rabbit antibodies were purchased

[1]To whom correspondence should be addressed. E-mail: rsakai@ncc.go.jp

doi: 10.1111/j.1349-7006.2009.01143.x

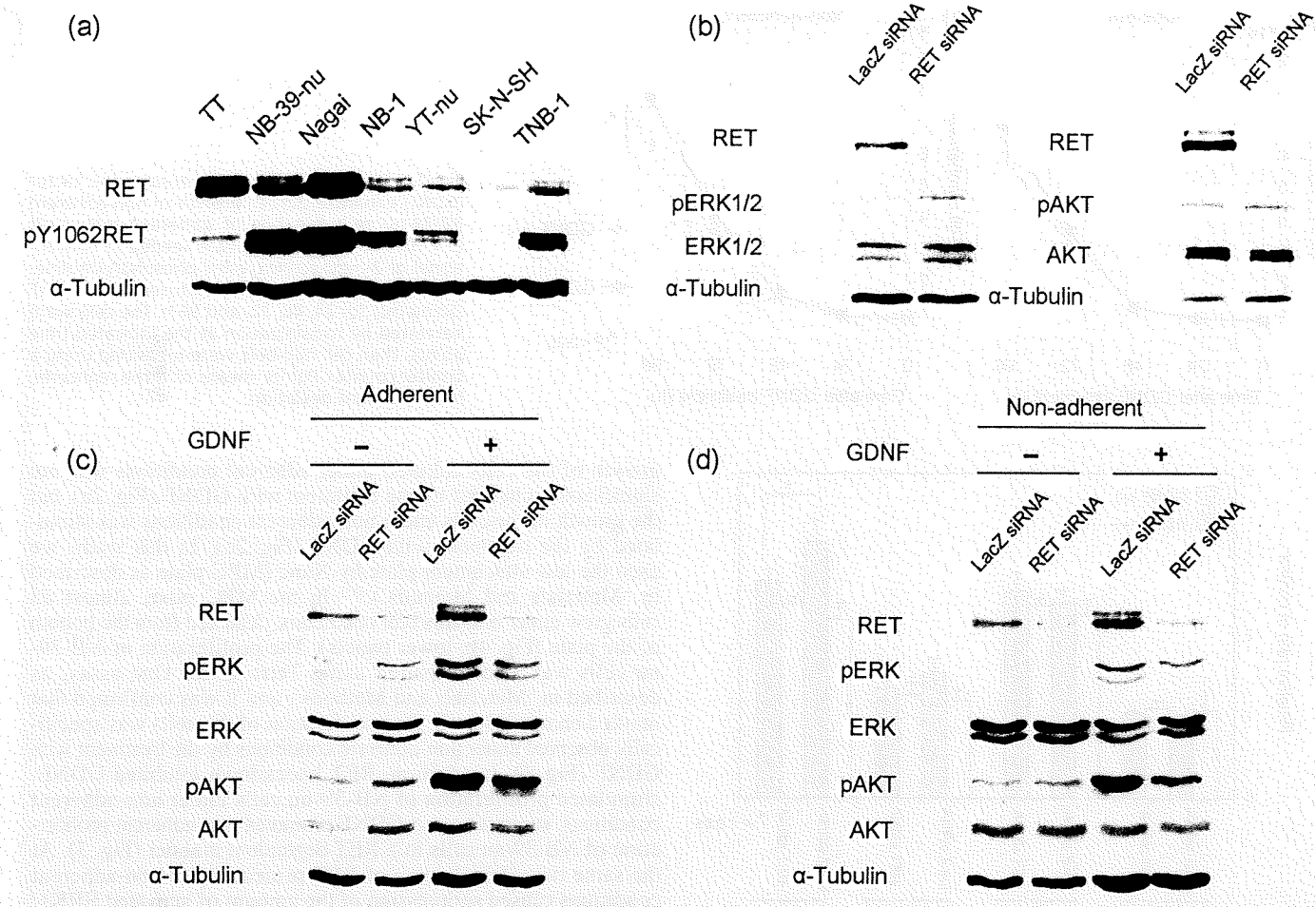

Fig. 1. (a) Expression of RET in various neuroblastoma cell lines. Exponentially growing neuroblastoma cell lines NB-39-nu, Nagai, NB-1, YT-nu, SK-N-SH, TNB-1, and a medullary thyroid carcinoma TT were harvested and the cell lysates subjected to Western blot analysis. (b) RET knockdown does not affect extracellular regulated kinase (ERK)1/2 or protein kinase B (AKT) signaling pathways in NB-39-nu cells. NB-39-nu cells (10×10^4/mL, 2 mL/well) were seeded in conventional 6-well plates in 10% fetal bovine serum containing RPMI-1640 medium, followed by treatment with LacZ short intefering RNA (siRNA) or RET siRNA at 0 h and 24 h, then harvested at 48 h for Western blot analysis. pAKT, phosphorylated AKT; pERK1/2, phosphorylated ERK1/2. (c, d) Glial cell line-derived neurotrophic factor (GDNF) enhances ERK1/2 and AKT signaling pathways in NB-39-nu cells in a RET-dependent manner. NB-39-nu cells (10×10^4/mL, 2 mL/well) were seeded in conventional 6-well plates in 10% fetal bovine serum containing RPMI-1640 medium, followed by treatment with LacZ siRNA or RET siRNA at 0 h and 24 h. After the cells were harvested at 48 h, the adherent cells were cultured with GDNF (50 ng/mL) for 24 h in conventional 6-well plates (c), while the non-adherent cells were cultured in 2-methacryloxyethyl phosphorylcholine-treated 6-well plates (d). The treatment was terminated at 72 h by harvesting the cells for Western blot analysis.

from Amersham Pharmacia (Little Chalfont, UK). Human recombinant GDNF was purchased from Sigma.

Cell proliferation assay. Cell proliferation was analyzed by Tetra Color One (Seikagaku, Tokyo, Japan) according to the manufacturer's instructions. Briefly, 3×10^3 or 1×10^4 cells/well were seeded in normal or low-cell-binding 96-well plates treated with 2-methacryloxyethyl phosphorylcholine (MPC; Nalge Nunc International, Tokyo, Japan). The cells were cultured for 24 or 48 h with or without GDNF (50 ng/mL) then subjected to Tetra Color for 3 h, followed by measurement for proliferation. The absorbance of the samples was measured at 450 nm on a microplate reader model 550 (Bio-Rad, Hercules, CA, USA).

Western blot analysis. The cell lysates were separated using sodium dodecyl sulfate–polyacrylamide gel electrophoresis, and transferred to a polyvinylidene difluoride membrane (Immobilon-P; Millipore, Bedford, MA, USA). After blocking of the membrane with blocking buffer (5% skim milk in Tris buffered saline containing 0.1% Tween-20), the membrane was probed with antibodies for detection. The membrane was further probed with horseradish peroxidase-conjugated anti-rabbit or anti-mouse IgG to visualize the reacted antibody.

Results

Expression of RET in various neuroblastoma cell lines. We first estimated the levels of the expression and phosphorylation of RET in various neuroblastoma cell lines and compared the estimated levels with those of the TT medullary thyroid carcinoma cell line, which carries C634W gain-of-function mutation of RET. Although RET was expressed in all six neuroblastoma cell lines, the levels of expression and phosphorylation of RET greatly varied among cell lines (Fig. 1a). Among the six neuroblastoma cell lines evaluated, two cell lines, NB-39-nu and Nagai, showed a high level of expression and phosphorylation of RET, which were comparable to or higher than those of TT.

GDNF enhances ERK1/2 and AKT signaling pathways in adherent NB-39-nu cells in a RET-dependent manner. We next knocked down RET expression to see the effect of activated RET signaling in NB-39-nu cells, one of the two neuroblastoma cell lines that showed a remarkable level of RET expression. As shown in Figure 1(b), RET expression was dramatically suppressed by treatment using RET RNAi, whereas phosphorylation of ERK1/2 and AKT, which have been reported to be universal downstream targets of receptor

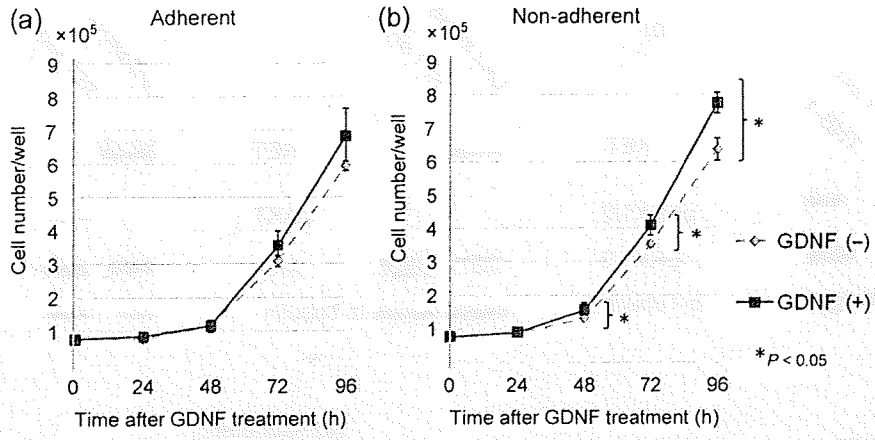

Fig. 2. Glial cell line-derived neurotrophic factor (GDNF) enhances the cell growth of non-adherent NB-39-nu cells but not of adherent cells. Cells (3×10^4/mL, 2.5 mL/well) were seeded in conventional or 2-methacryloxyethyl phosphorylcholine-treated 6-well plates, and cultured with GDNF (50 ng/mL) for 24, 48, 72, and 96 h. The cells were harvested by trypsinization at the indicated time points, then cell numbers were measured using a Coulter counter. Points, means of three replicates; bars, standard deviation.

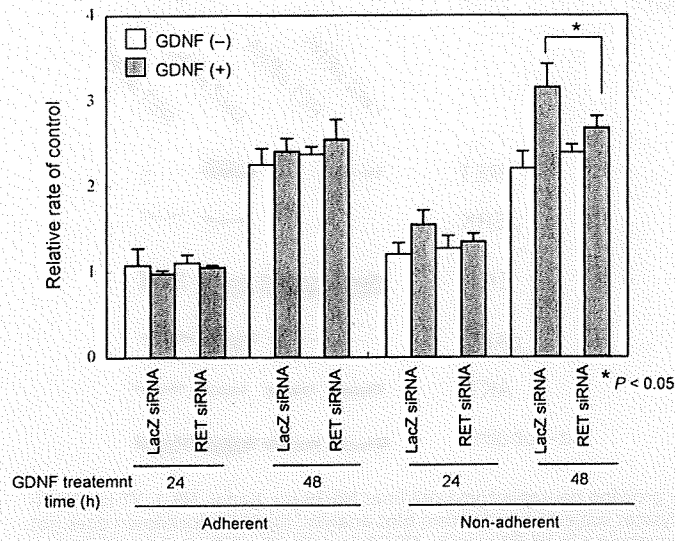

Fig. 3. RET knockdown abrogates glial cell line-derived neurotrophic factor (GDNF)-stimulated proliferation of non-adherent NB-39-nu neuroblastoma cells. NB-39-nu cells (10×10^4/mL, 2 mL/well) were seeded in conventional 6-well plates in 10% fetal bovine serum containing RPMI-1640 medium, followed by treatment with LacZ short interfering RNA (siRNA) or RET siRNA at 0 h and 24 h. At 48 h, the cells were harvested and seeded (3×10^3/mL, 0.1 mL/well) in conventional or 2-methacryloxyethyl phosphorylcholine-treated 96-well plates with or without GDNF (50 ng/mL) for 24 or 48 h. Cell proliferations were determined at the indicated time points. Columns, means of three replicates; bars, standard deviation.

tyrosine kinases including RET, were not significantly affected. This suggests that these downstream signaling pathways are not under the regulation of activated RET under normal culture conditions. However, phosphorylation of ERK1/2 and AKT were significantly enhanced by GDNF treatment in the existence of serum, as indicated in Figure 1(c), and this enhancement was inhibited by the knockdown of RET protein, indicating that ERK1/2 and AKT signals were activated by the stimulation with GDNF in a RET-dependent manner in this cell line. Phosphorylation of AKT and ERK1/2 was also increased by stimulation of GDNF in the serum-depleted condition after serum starvation, and the increased phosphorylation of AKT was inhibited by RET knockdown, whereas the inhibition of the increased phosphorylation of ERK1/2 by RET knockdown was not obvious (Fig. S1).

GDNF enhances cell proliferation of non-adherent NB-39-nu cells but not of adherent cells. As RET downstream signaling was stimulated by the treatment of GDNF in NB-39-nu cells, we next examined the effect of GDNF on the proliferation of NB-39-nu cells. The growth of the cells cultured under adherent conditions was not significantly changed by the treatment with GDNF (Fig. 2a), but the growth of the cells under non-adherent conditions was stimulated by the treatment with GDNF (Fig. 2b). In this study, we used the low attachment plate by Nunc (MPC plate as described in 'Materials and Methods').[25] In the MPC plate, almost all cells grew under non-adherent conditions, detached from the bottom of the plate (Fig. 4b, lower panels). The proliferation of NB-39-nu cells was also measured using Tetra Color One assay, as described in 'Materials and Methods', and it was confirmed that marked enhancement in the proliferation of the cells was specifically observed under non-adherent conditions by the treatment with GDNF (Fig. 3). In addition, RET knockdown inhibited GDNF-stimulated proliferation of NB-39-nu cells under non-adherent conditions, suggesting that GDNF promotes non-adherent proliferation of NB-39-nu cells in a RET-dependent manner (Fig. 3). At the same time, knockdown of RET protein under non-adherent conditions caused suppression of the amount of activated ERK1/2 and ATK (Fig. 1d).

In addition to NB-39-nu cells, another neuroblastoma cell line, NB-1, was evaluated for proliferation when treated with GDNF with or without of RET knockdown. Like NB-39-nu cells, the proliferation of NB-1 cells was enhanced by GDNF under non-adherent conditions, but not under adherent conditions, and the enhancement was inhibited by RET knockdown (Fig. S2).

GDNF does not induce neuronal differentiation markers in NB-39-nu cells. It has been shown that GDNF induces cell differentiation in most primary neuroblastoma tissues, which generally results in the inhibition of the proliferation of cancer cells, so we investigated whether differentiation was induced by GDNF treatment of NB-39-nu cells by monitoring two neuronal markers, GAP-43 and chromogranin-A. The treatment did not cause upregulation of these markers at a protein level, under either adherent or non-adherent conditions (Fig. 4a). In addition, no obvious morphological changes, such as neurite outgrowth, were observed with the addition of GDNF under adherent conditions (Fig. 4b, upper panels). These findings suggest that the treatment of GDNF did not induce neuronal differentiation under the experimental conditions. Furthermore, the cells showed evidence of cluster formations under non-adherent conditions, and the clusters of the cells treated with GDNF appeared to be significantly larger (Fig. 4b, lower panels).

Discussion

It has been shown that RET is expressed in most neuroblastoma cell lines and tissues, although its role in neuroblastoma remains to be determined. In this study, we analyzed the role of RET protein in neuroblastoma using NB-39-nu cells in which especially high levels of expression and tyrosine phosphorylation of RET

doi: 10.1111/j.1349-7006.2009.01143.x

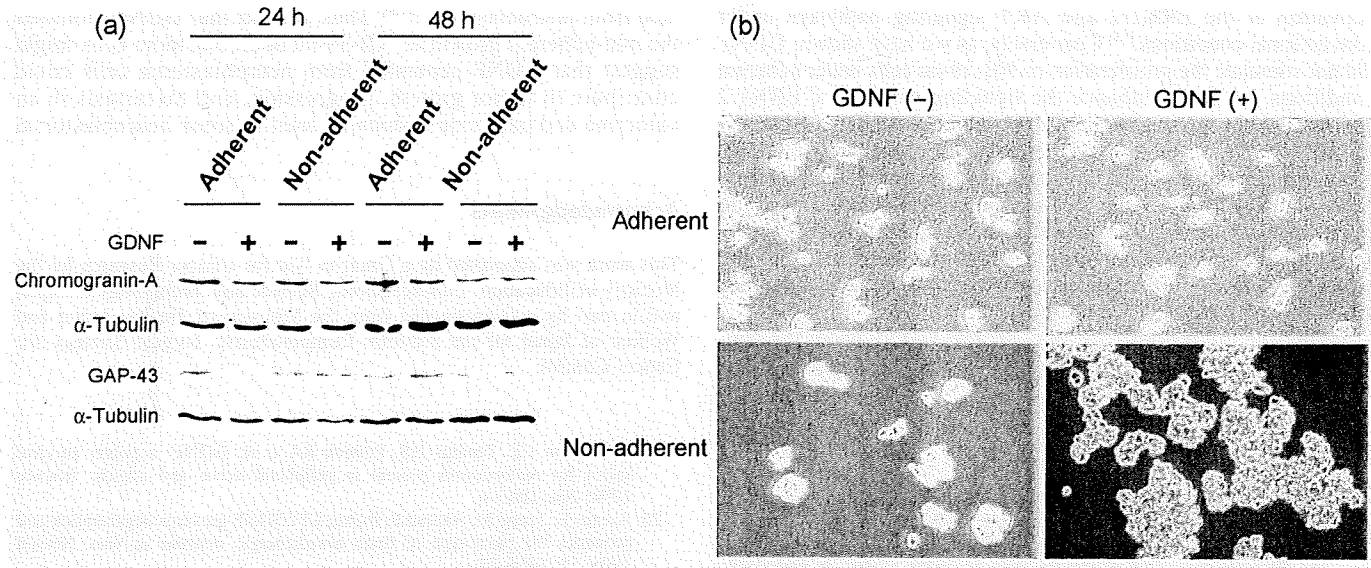

Fig. 4. GDNF does not induce neuronal differentiation markers or morphological change in adherent NB-39-nu cells. NB-39-nu cells (10×10^4/mL, 2 mL/well) were seeded in conventional or 2-methacryloxyethyl phosphorylcholine-treated 6-well plates in 10% fetal bovine serum containing RPMI-1640 medium with or without glial cell line-derived neurotrophic factor (GDNF; 50 ng/mL) for 24 or 48 h. (a) The cells were harvested for Western blot analysis at 24 h and 48 h. (b) Microscopic appearance of NB-39-nu cells cultured with or without GDNF under adherent or non-adherent conditions at 48 h.

protein were observed. In two of the six cell lines examined, NB-39-nu and Nagai cells, the expression and phosphorylation levels of RET protein were comparable to or higher than those of TT cells. TT cells are derived from medullary thyroid carcinoma, and were found to harbor C634W gain-of-function mutation of RET. It was considered that activation of RET caused by gain-of-function mutation, which led to constitutive activation of downstream signaling, is responsible for oncogenesis in TT cells. Actually, it has been shown that the inhibition of RET signaling by expressing a dominant negative form of RET leads to suppression of ERK1/2 and AKT and the proliferation in TT cells, suggesting that the activated RET plays an important role in proliferation.[26,27] Although RET protein shows high levels of tyrosine phosphorylation in NB-39-nu and Nagai cells without any known mutations, the proliferation and downstream signaling of RET were not inhibited by RET RNAi of NB-39-nu cells under normal culture conditions in this study.

However, ERK1/2 and AKT, downstream molecules of RET protein, were further activated upon the stimulation of its ligand, GDNF, in a RET-dependent manner, suggesting a ligand-dependent nature as a wild-type RET protein. Nevertheless, the proliferation of the cells under adherent conditions was not stimulated by the treatment with GDNF. Interestingly, the proliferation of NB-39-nu cells was stimulated by GDNF treatment under non-adherent conditions, and this was suppressed by RET siRNA. These results suggest that GDNF promotes non-adherent proliferation of NB-39-nu cells in a RET-dependent manner. Similar results of the effect of GDNF on proliferation were observed in another neuroblastoma cell line, NB-1, suggesting that the phenomenon of RET-dependent GDNF-induced increase of proliferation under non-adherent conditions was not exclusive to NB-39-nu cells.

We noticed that RET knockdown had an obvious inhibitory effect on the activation of both ERK1/2 and AKT in long-term stimulation (24 h) by GDNF in the existence of serum, but it had little inhibitory effect on the activation of ERK1/2 in rapid stimulation (15 min) by GDNF after serum starvation, suggesting a special mechanism of long-term activation of ERK1/2 by GDNF-RET signaling.

When the NB-39-nu cells were cultured in non-adherent conditions, they grew in cluster formations, as shown in Figure 4(b). It has been shown that intercellular adhesion under non-adherent conditions generates the stimulations that support survival and proliferation in some cell lines.[28,29] GDNF might enhance this intercellular stimulation generated by cluster formation of the cells, resulting in promotion of the proliferation of the cells. In the metastasis cascade, it can be considered to be a critical step that the metastasizing cancer cells become detached from the extracellular matrix and survive and proliferate in touch with adjacent cancer cells, suggesting the possibility that GDNF-RET signaling might promote cancer metastasis by facilitating this step.[30,31]

It has been shown that GDNF induces differentiation in most neuroblastoma tissues by the primary culture system.[17] Therefore, we initially suspected that the loss of the growth promotion effect of GDNF under adherent conditions was due to its induction of differentiation. However, GDNF stimulation did not cause either induction of neuronal markers, such as GAP-43 and chromogranin-A, nor morphological changes such as neurite outgrowth, suggesting that neuronal differentiation was not induced by the treatment of GDNF in NB-39-nu cells under adherent conditions.

We previously demonstrated that anaplastic lymphoma kinase (ALK) was overexpressed and activated by gene amplification in NB-39-nu cells, and found that the AKT and ERK1/2 signals were significantly blocked by the knockdown of ALK,[32,33] suggesting that activation of ALK dominates the growth and survival signaling in this cell line. Thus, it is possible that the growth of NB-39-nu cells under GDNF-free conditions, or under adherent conditions, is mainly sustained by activated ALK. This is also the case with NB-1 overexpressing ALK. Furthermore, we observed that the proliferations in other neuroblastoma cell lines, TNB-1 and YT-nu, which are not overexpressing ALK were enhanced by GDNF under both adherent and non-adherent conditions (data not shown), suggesting that the cell proliferation might be dominantly regulated by activated ALK which overcomes GDNF-RET signaling under adherent conditions in NB-39-nu and NB-1 cells. GDNF-RET signaling might have a special role in non-adherent growth that might not be supported by signals from other growth factor receptors, including ALK.

It was previously reported that the proliferation of SH-SY5Y neuroblastoma cell line was enhanced by GDNF with the

activation of the ERK1/2 and AKT signaling pathways under conventional conditions.[34] Conversely, as we have shown, GDNF did not stimulate the proliferation of NB-39-nu cells under adherent conditions, but it did enhance the signaling pathway of ERK1/2 and AKT. Although the mechanism by which the differential ability of GDNF to proliferate the cells between these two cell lines remains to be elucidated, the dominant influence of the activated ALK pathway in NB-39-nu cells is naturally suspected. It could be postulated that other pathways such as the signal from NCAM,[35] also a receptor for GNDF, might contribute differently to the signaling pathway for proliferation between these two cell lines growing under adherent conditions.

Various neuroblastoma cell lines secrete GDNF under the controls of various cytokines and growth factors that are also generated from neuroblastoma.[17,36] Thus, the fact that GDNF promotes the non-adherent growth of NB-39-nu neuroblastoma cells might suggest that GDNF generated from neuroblastoma cells could contribute to tumor growth, progression, and metastasis in an autocrine and paracrine fashion, at least in some neuroblastoma.

Acknowledgments

This work was supported by a Grant-in Aid for Cancer Research by the Ministry of Education, Culture, Sports, Science and Technology of Japan and in part by a Grant-in-Aid from the Ministry of Health, Labor and Welfare of Japan for the 3rd-term Comprehensive 10-year Strategy for Cancer Control.

References

1 Pachnis V, Mankoo B, Costantini F. Expression of the c-ret proto-oncogene during mouse embryogenesis. Development 1993; 119: 1005–17.
2 Tsuzuki T, Takahashi M, Asai N, Iwashita T, Matsuyama M, Asai J. Spatial and temporal expression of the ret proto-oncogene product in embryonic, infant and adult rat tissues. Oncogene 1995; 10: 191–8.
3 Jain S, Naughton CK, Yang M et al. Mice expressing a dominant-negative Ret mutation phenocopy human Hirschsprung disease and delineate a direct role of Ret in spermatogenesis. Development 2004; 131: 5503–13.
4 Donis KH, Dou S, Chi D et al. Mutations in the RET proto-oncogene are associated with MEN 2A and FMTC. Hum Mol Genet 1993; 2: 851–6.
5 Mulligan LM, Kwok JB, Healey CS et al. Germ-line mutations of the RET proto-oncogene in multiple endocrine neoplasia type 2A. Nature 1993; 363: 458–60.
6 Hofstra RM, Landsvater RM, Ceccherini I et al. A mutation in the RET proto-oncogene associated with multiple endocrine neoplasia type 2B and sporadic medullary thyroid carcinoma. Nature 1994; 367: 375–6.
7 Eng C, Mulligan LM, Smith DP et al. Mutation of the RET protooncogene in sporadic medullary thyroid carcinoma. Genes Chromosomes Cancer 1995; 12: 209–12.
8 Eng C, Smith DP, Mulligan LM et al. A novel point mutation in the tyrosine kinase domain of the RET proto-oncogene in sporadic medullary thyroid carcinoma and in a family with FMTC. Oncogene 1995; 10: 509–13.
9 Grieco M, Santoro M, Berlingieri MT et al. PTC is a novel rearranged form of the ret proto-oncogene and is frequently detected in vivo in human thyroid papillary carcinomas. Cell 1990; 60: 557–63.
10 Bongarzone I, Monzini N, Borrello MG et al. Molecular characterization of a thyroid tumor-specific transforming sequence formed by the fusion of ret tyrosine kinase and the regulatory subunit RIα of cyclic AMP-dependent protein kinase A. Mol Cell Biol 1993; 13: 358–66.
11 Edery P, Lyonnet S, Mulligan LM et al. Mutations of the RET proto-oncogene in Hirschsprung's disease. Nature 1994; 367: 378–80.
12 Romeo G, Ronchetto P, Luo Y et al. Point mutations affecting the tyrosine kinase domain of the RET proto-oncogene in Hirschsprung's disease. Nature 1994; 367: 377–8.
13 Brodeur GM. Neuroblastoma: biological insights into a clinical enigma. Nat Rev Cancer 2003; 3: 203–16.
14 Nagao M, Ishizaka Y, Nakagawara A et al. Expression of ret proto-oncogene in human neuroblastomas. Jpn J Cancer Res 1990; 81: 309–12.
15 Ikeda I, Ishizaka Y, Tahira T et al. Specific expression of the ret proto-oncogene in human neuroblastoma cell lines. Oncogene 1990; 5: 1291–6.
16 Borrello MG, Bongarzone I, Pierotti MA et al. trk and ret proto-oncogene expression in human neuroblastoma specimens: high frequency of trk expression in non-advanced stages. Int J Cancer 1993; 54: 540–5.
17 Hishiki T, Nimura Y, Isogai E et al. Glial cell line-derived neurotrophic factor/neurturin-induced differentiation and its enhancement by retinoic acid in primary human neuroblastomas expressing c-Ret, GFRα-1, and GFRα-2. Cancer Res 1998; 58: 2158–65.
18 Lin LF, Doherty DH, Lile JD, Bektesh S, Collins F. GDNF: a glial cell line-derived neurotrophic factor for midbrain dopaminergic neurons. Science 1993; 260: 1130–2.
19 Henderson CE, Phillips HS, Pollock RA et al. GDNF: a potent survival factor for motoneurons present in peripheral nerve and muscle. Science 1994; 266: 1062–4.
20 Arenas E, Trupp M, Akerud P, Ibanez CF. GDNF prevents degeneration and promotes the phenotype of brain noradrenergic neurons in vivo. Neuron 1995; 15: 1465–73.
21 Arighi E, Borrello MG, Sariola H. RET tyrosine kinase signaling in development and cancer. Cytokine Growth Factor Rev 2005; 16: 441–67.
22 Hayashi H, Ichihara M, Iwashita T et al. Characterization of intracellular signals via tyrosine 1062 in RET activated by glial cell line-derived neurotrophic factor. Oncogene 2000; 19: 4469–75.
23 Ishikawa S, Ohshima Y, Suzuki T, Oboshi S. Primitive neuroectodermal tumor (neuroepithelioma) of spinal nerve root – Report of an adult case and establishment of a cell line. Acta Pathol Jpn 1979; 29: 289–301.
24 Kuga N, Yoshida K, Seido T et al. Heterotransplantation of cultured human cancer cells and human cancer tissues into nude mice. Gann 1975; 66: 547–60.
25 Uekita T, Jia L, Narisawa-Saito M, Yokota J, Kiyono T, Sakai R. CUB domain-containing protein 1 is a novel regulator of anoikis resistance in lung adenocarcinoma. Mol Cell Biol 2007; 27: 7649–60.
26 Drosten M, Stiewe T, Putzer BM. Antitumor capacity of a dominant-negative RET proto-oncogene mutant in a medullary thyroid carcinoma model. Hum Gene Ther 2003; 14: 971–82.
27 Drosten M, Hilken G, Bockmann M et al. Role of MEN2A-derived RET in maintenance and proliferation of medullary thyroid carcinoma. J Natl Cancer Inst 2004; 96: 1231–9.
28 Bates RC, Edwards NS, Yates JD. Spheroids and cell survival. Crit Rev Oncol Hematol 2000; 36: 61–74.
29 Lawlor ER, Scheel C, Irving J, Sorensen PH. Anchorage-independent multicellular spheroids as an in vitro model of growth signaling in Ewing tumors. Oncogene 2002; 21: 307–18.
30 Volk T, Geiger B, Raz A. Motility and adhesive properties of high- and low-metastatic murine neoplastic cells. Cancer Res 1984; 44: 811–24.
31 Nabi IR, Raz A. Loss of metastatic responsiveness to cell shape modulation in a newly characterized B16 melanoma adhesive cell variant. Cancer Res 1988; 48: 1258–64.
32 Miyake I, Hakomori Y, Misu Y et al. Domain-specific function of ShcC docking protein in neuroblastoma cells. Oncogene 2005; 24: 3206–15.
33 Osajima-Hakomori Y, Miyake I, Ohira M, Nakagawara A, Nakagawa A, Sakai R. Biological role of anaplastic lymphoma kinase in neuroblastoma. Am J Pathol 2005; 167: 213–22.
34 Hirata Y, Kiuchi K. Mitogenic effect of glial cell line-derived neurotrophic factor is dependent on the activation of p70S6 kinase, but independent of the activation of ERK and up-regulation of Ret in SH-SY5Y cells. Brain Res 2003; 983: 1–12.
35 Paratcha G, Ledda F, Ibanez CF. The neural cell adhesion molecule NCAM is an alternative signaling receptor for GDNF family ligands. Cell 2003; 113: 867–79.
36 Verity AN, Wyatt TL, Lee W et al. Differential regulation of glial cell line-derived neurotrophic factor (GDNF) expression in human neuroblastoma and glioblastoma cell lines. J Neurosci Res 1999; 55: 187–97.

Supporting Information

Additional Supporting Information may be found in the online version of this article:

Fig. S1. Glial cell line-derived neurotrophic factor (GDNF)-induced enhancement of extracellular regulated kinase (ERK)1/2 and protein kinase B (AKT) signaling in serum-depleted conditions in NB-39-nu neuroblastoma cells. NB-39-nu cells (10×10^4/mL, 2 mL/well) were seeded in conventional 6-well plates in 10% fetal bovine serum containing RPMI-1640 medium, followed by treatment with LacZ short interfering RNA

doi: 10.1111/j.1349-7006.2009.01143.x

(siRNA) or RET siRNA at 0 h and 24 h, then harvested at 48 h. After culturing the cells in serum-depleted condition for 24 h under adherent conditions, the cells were treated with GDNF (50 ng/mL) in serum-depleted conditions for 15 min, then harvested for Western blot analysis.

Fig. S2. RET knockdown abrogates glial cell line-derived neurotrophic factor (GDNF)-stimulated proliferation of non-adherent NB-1 neuroblastoma cells. NB-1 cells (10×10^4/mL, 2 mL/well) were seeded in conventional 6-well plates in 10% fetal bovine serum containing RPMI-1640 medium, followed by treatment with LacZ short interfering RNA (siRNA) or RET siRNA at 0 h and 24 h. At the 48 h time point, the cells were harvested and seeded (1×10^4/mL, 0.1 mL/well) in conventional or 2-methacryloxyethyl phosphorylcholine-treated 96-well plates in 10% fetal bovine serum containing RPMI-1640 medium with or without GDNF (50 ng/mL) for 24 or 48 h. RET knockdown was confirmed for the cells harvested at 48 h by Western blot analysis. Cell proliferations were determined at the indicated time points by Tetra Color One assay as described in Materials and Methods. Columns, means of three replicates; bars, standard deviation.

Association of Estrogen Receptor α and Histone Deacetylase 6 Causes Rapid Deacetylation of Tubulin in Breast Cancer Cells

Kotaro Azuma,[1] Tomohiko Urano,[1,2] Kuniko Horie-Inoue,[4] Shin-ichi Hayashi,[5] Ryuichi Sakai,[3] Yasuyoshi Ouchi,[1] and Satoshi Inoue[1,2,4]

Departments of [1]Geriatric Medicine and [2]Anti-Aging Medicine, Graduate School of Medicine, The University of Tokyo and [3]Growth Factor Division, National Cancer Center Research Institute, Tokyo, Japan; [4]Division of Gene Regulation and Signal Transduction, Research Center for Genomic Medicine, Saitama Medical School, Saitama, Japan; and [5]Department of Medical Technology, Course of Health Sciences, School of Medicine, Tohoku University, Miyagi, Japan

Abstract

Estrogen receptor α (ERα) is a nuclear receptor that functions as a ligand-activated transcription factor. Besides its genomic action in nuclei, ERα could exert nongenomic actions at the plasma membrane. To investigate the mechanism underlying the nongenomic action of ERα in breast cancer cells, we generated a construct of membrane-targeted ERα (memER), an expression vector of ERα without the nuclear localizing signal and including instead the membrane-targeting sequence of Src kinase. MemER was stably expressed in human breast cancer MCF-7 cells. Cell migration test and tumorigenic assay in nude mice revealed that the *in vitro* motility and the *in vivo* proliferation activity of MCF-7 cells expressing memER were significantly enhanced compared with those of vector-transfected cells. Interestingly, the acetylation level of tubulin in memER-overexpressing cells was lower than that in control cells. We found that histone deacetylase (HDAC) 6 translocated to the plasma membrane shortly after estrogen stimulation, and rapid tubulin deacetylation subsequently occurred. We also showed that memER associated with HDAC6 in a ligand-dependent manner. Although tamoxifen is known for its antagonistic role in the ERα genomic action in MCF-7 cells, the agent showed an agonistic function in the memER-HDAC6 association and tubulin deacetylation. These findings suggest that ERα ligand dependently forms a complex with HDAC6 and tubulin at the plasma membrane. Estrogen-dependent tubulin deacetylation could provide new evidence for the nongenomic action of estrogen, which potentially contributes to the aggressiveness of ERα-positive breast cancer cells. [Cancer Res 2009;69(7):2935–40]

Introduction

Estrogen plays an essential role in various biological and pathologic processes, particularly in the development of breast cancer (1). Estrogen exerts its function by activating its corresponding nuclear receptor, estrogen receptor α (ERα). ERα is a ligand-dependent transcription factor that forms complexes with coactivators and histone acetyltransferases in response to agonists. The acetylation of histones changes the chromatin conformation and activates transcription pathways. In contrast, ERα forms complexes with corepressors and histone deacetylases (HDAC) in the treatment with antagonists. The deacetylation of histones alters the chromatin conformation into a transcriptionally inactive form. The expression status of ERα and its primary target progesterone receptor is important in the management of breast cancer, as ERα- and progesterone receptor–positive tumors are known to respond to antiestrogenic treatment. Tamoxifen has been used for years as a prototypic selective estrogen receptor modulator for endocrine therapy in breast cancer.

Recently, it has been shown that ERα has an alternative function that mediates specific signals through the association with molecules outside the nuclei, in addition to its known activity of transcriptional regulation (2). In vascular endothelial cells, estrogen rapidly induces nitric oxide production by activating the phosphatidylinositol-3-OH kinase pathway (3). In osteoblasts and fibroblasts, ERα mediates an antiapoptotic effect by activating the Src-Shc-Erk pathway, predominantly through the action of the activation function 2 domain (4). These phenomena are known as nongenomic actions, which may be distinct from the classic genomic actions of ERα because of their rapid time course and the subcellular localization of the molecules interacting with ERα.

Ligand-dependent rapid phosphorylation of MAP kinases, another example of nongenomic action by estrogen, has been also revealed in ERα-positive breast cancer MCF-7 cells (5). We showed previously that a subset of ERα in MCF-7 cells translocated to the plasma membrane in response to estradiol (E_2), and the activation function 1 (AF-1) domain of ERα interacted with polymerized tubulin when the AF-1 domain of ERα was expressed at the plasma membrane with the membrane-targeting signal (6).

Recently, HDAC6, a class IIB zinc-dependent HDAC predominantly localized in the cytoplasm, has been shown to deacetylate tubulin (7). Tubulin is the major component of microtubules, which play a critical role in the cell migration, cell morphology, cell-cell interaction, and tumor metastasis. In breast cancer, HDAC6 expression was induced in response to estrogen, and HDAC6 overexpression was reported as a poor prognostic factor (8). It has been also shown that the motility of breast cancer cells could be enhanced by HDAC6 overexpression and reduced by the inhibition of HDAC6 activity (9).

In the present study, we show a novel nongenomic action of estrogen in breast cancer cells, as the membrane-localized ERα associates with HDAC6 and causes rapid deacetylation of tubulin in a ligand-dependent manner.

Materials and Methods

Antibodies and reagents. Anti-Myc, anti-ERα (H-184), anti-HDAC6, and anti-HA polyclonal antibodies were purchased from Santa Cruz Biotechnology. Anti-FLAG M2 and M5 monoclonal, anti-α-tubulin (B-5-1-2), and anti-acetylated-α-tubulin (6-11B-1) antibodies were purchased from

Requests for reprints: Satoshi Inoue, Department of Geriatric Medicine, Graduate School of Medicine, The University of Tokyo, 7-3-1 Hongo, Bunkyo-ku, Tokyo 113-8655, Japan. Phone: 81-3-5800-8652; Fax: 81-3-5800-6530; E-mail: INOUE-GER@h.u-tokyo.ac.jp.

doi:10.1158/0008-5472.CAN-08-3458

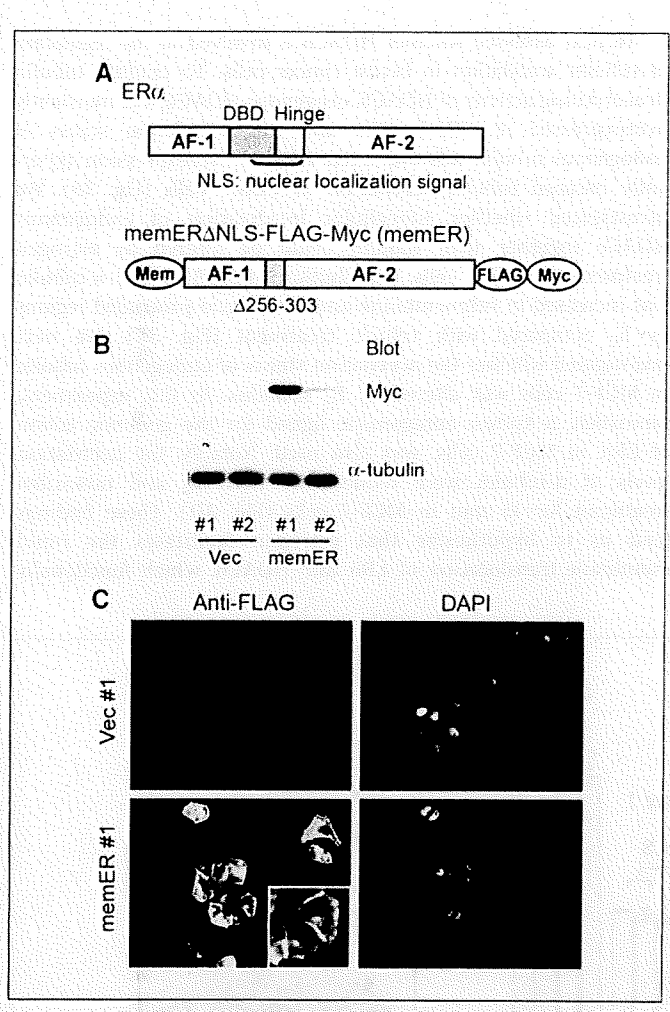

Figure 1. Generation of MCF-7 cells stably expressing memER. *A*, schematic representation of full-length ERα and memER. *B*, Western blot analysis of MCF-7 cells stably expressing memER (*memER #1* and *#2*) and vector clones (*vec #1* and *#2*). Whole cell lysates were immunoblotted with anti-Myc and anti–α-tubulin antibodies. *C*, immunocytochemistry of MCF-7 clones expressing vec #1 and memER #1. Immunostaining with anti-FLAG (*M2*) antibody shows membrane localization of ERα protein in memER #1 clone. DAPI staining shows the cell nuclei. Cells were visualized with fluorescence microscopy at a ×600 magnification. The memER #1 clone stained with anti-FLAG antibody is enlarged in the inset.

SIGMA. Alexa Fluor 488 goat anti-mouse IgG and Alexa Fluor 594 goat anti-rabbit IgG were purchased from Molecular Probe. Horseradish peroxidase–conjugated anti-mouse and anti-rabbit antibodies were purchased from Amersham Pharmacia. 17β-estradiol (E_2) and tamoxifen were purchased from SIGMA. HA-peptide was purchased from Roche.

Plasmids. Membrane-targeted ERα (memER) with FLAG and Myc epitope tags (memERΔNLS-FLAG-Myc, memER) was generated in two steps. In the first step, an expression construct of ERα with an NH_2-terminal membrane–targeting sequence (derived from the NH_2 terminus of Src kinase; MGSNKSKPKDASQ) and COOH-terminal FLAG and Myc tags was generated. In the second step, the sequence coding the nuclear localizing signal (NLS, 256-303 amino acids of ERα; ref. 10) was deleted with PCR-based sited-directed mutagenesis from the plasmid generated in the first step. The AF-1 and activation function 2 domains of ERα with the NH_2-terminal membrane–targeting sequence and COOH-terminal FLAG tag (memAF1 and memAF2, respectively) were generated as previously described (6). Deletion mutants of HDAC6 with the COOH-terminal HA tag were generated by inserting HDAC6 amplicons in pcDNA3.1(−)/Myc-His B, including the following amino acid numbers of the HDAC protein as follows: full-length HDAC6 (full), 1-1215; ΔZnF, 1-998; ΔDD2-ZnF, 1-408; ΔDD1, 409-1215; ΔDD1-DD2, 999-1215.

Cell culture and transfection. MCF-7, COS-7, and HEK293T cells were maintained in DMEM with 10% FCS at 37°C under 5% CO_2. MCF-7 and 293T cells were cultured in estrogen-starved medium (phenol red–free DMEM with 5% charcoal/dextran-treated FCS) for 2 d before E_2/tamoxifen treatment. Transfection was performed using FuGENE 6 (Roche). To establish stable transfectants, MCF-7 clones were selected using G418 (SIGMA) at a concentration of 800 μg/mL.

Immunoblotting and immunoprecipitation. Immunoblotting and immunopreciptation were performed as previously described (6). For immunoprecipitation with the anti-HA antibody, aliquots of protein were mixed with anti-HA agarose conjugate (SIGMA).

Immunocytochemistry. Immunocytochemical analysis was performed as described (6). Nuclei were stained with 4′,6-diamidino-2-phenylindole (DAPI; SIGMA) diluted with PBS (1:10,000) for 10 min. Cells were visualized with a fluorescence microscope (KEYENCE) or Radiance 2100 confocal microscope (BIO-RAD).

Cell migration assay. The cell migration assay was performed as previously described (11). The number of MCF-7 cells migrating through a polyethylene terephthalate filter with 8-μm pores (Becton Dickinson) in 24 h was counted under microscopic examination.

Cell proliferation assay. Cells were seeded in 96-well plates at a density of 1,000 cells per well. The viable cell number was quantified using tetrazolium salt (WST-8) that could be converted to a water-soluble formazan by metabolically active cells. Spectrophotometric absorbance for formazan dye was measured at 450 nm, with absorbance at 655 nm as reference.

***In vivo* tumor growth assay.** The *in vivo* tumor growth assay was basically performed as previously described (12). Four-week-old female BALB/c nude mice were ovariectomized, and a 17β-estradiol pellet (0.72 mg; 90-d release; Innovative Research of America) was s.c. transplanted in the right shoulder of each mouse. For s.c. implantation of tumor cells, 1 million cells suspended in 100 μL of DMEM with 5% FCS were mixed with Matrigel and implanted in the left shoulder of ovariectomized nude mice. Tumor size was weekly measured at 2 to 6 wk after implantation, and tumor volume was determined using the tumor radius. Relative tumor volume was determined by normalizing to the mean value at 2 wk after implantation.

Statistical analyses. Differences between the mean values of memER-expressing MCF-7 clones and vector-expressing clones were analyzed using the Student's *t* test.

Results

Establishment of cell lines stably expressing memER. To analyze the function of membrane-localized ERα, we generated an expression vector of memER that contains the NH_2-terminal membrane-localizing sequence derived from Src kinase and lacks the NLS (Fig. 1*A*; ref. 10). Src kinase is a nonreceptor tyrosine kinase localizing at the plasma membrane with its myristoylated NH_2-terminal sequence. We established breast cancer MCF-7 cells stably expressing memER and the control vector (Fig. 1*B*). Immunocytochemical staining revealed that memER was predominantly expressed at the plasma membrane (Fig. 1*C*).

Enhanced motility and *in vivo* tumorigenesis of MCF-7 cells stably expressing memER. To elucidate the function of membrane-localized ERα, the motility of MCF-7 clones stably expressing memER and control vector was evaluated. The number of cells migrating through the 8-μm-pored polyethylene terephthalate filter in 24 h was counted. The motility of memER overexpressing MCF-7 cells (*memER #1* and *#2*) was significantly higher than that of vector clones (*vec #1* and *#2*; Fig. 2*A*). To exclude the possibility that the difference in the growth affected the cell migration, the growth rate of each clone was measured. The growth rates of memER overexpressing clones had not apparently increased

compared with control cells (Fig. 2*B*). Next, we investigated the contribution of membrane-localized ER to *in vivo* tumorigenesis by using a nude mouse xenograft model. To avoid the effect of endogenous estrogen production, nude mice were ovariectomized and estrogen pellets were inserted s.c. The results showed that tumors derived from memER clones (*memER #1* and *#2*) were larger than those from vector clones (*vec #1* and *#2*; Fig. 2*C* and *D*). Taken together, these results indicate that the overexpression of memER facilitates cell migration activity in cultured cells as well as *in vivo* tumor formation of breast cancer cells.

Rapid tubulin deacetylation as a novel nongenomic action of estrogen. We have previously revealed that tubulin could associate with the membrane-targeted AF-1 domain of ERα in MCF-7 cells (6). Tubulin is an important component of the microtubule network that regulates cell motility, which could be enhanced by HDAC6 that deacetylates tubulin (7). Thus, we investigated whether memER overexpression could modulate the acetylation status of tubulin in MCF-7 cells. Tubulin acetylation was reduced in memER-expressing clones compared with vector clones (Fig. 3*A*).

We next assessed whether HDAC6 is involved in the regulation of tubulin acetylation in breast cancer cells. To confirm tubulin deacetylating activity of HDAC6, exogenous HDAC6 was transiently overexpressed in COS-7 cells and the acetylation status of endogenous tubulin was evaluated. HDAC6 overexpression apparently reduced tubulin acetylation in COS-7 cells (Fig. 3*B*). We investigated whether subcellular localization of endogenous HDAC6 together with tubulin could be altered by estrogen treatment in MCF-7 cells. Distribution of HDAC6 and α-tubulin was increased in submembrane and membrane protruded regions by E_2 compared with vehicle treatment (Fig. 3*C*). We next investigated whether the acetylation status of endogenous tubulin in MCF-7 cells was altered by E_2 stimulus. In this experiment, tamoxifen, a known antagonistic ligand for the genomic action of ERα in MCF-7 cells, was also used. Notably, the acetylation levels of α-tubulin were reduced by both E_2 and tamoxifen treatment for 15 min in MCF-7 cells (Fig. 3*D*). These findings lead us to hypothesize that estrogen facilitates the rapid membrane translocation of ERα and HDAC6, which functionally

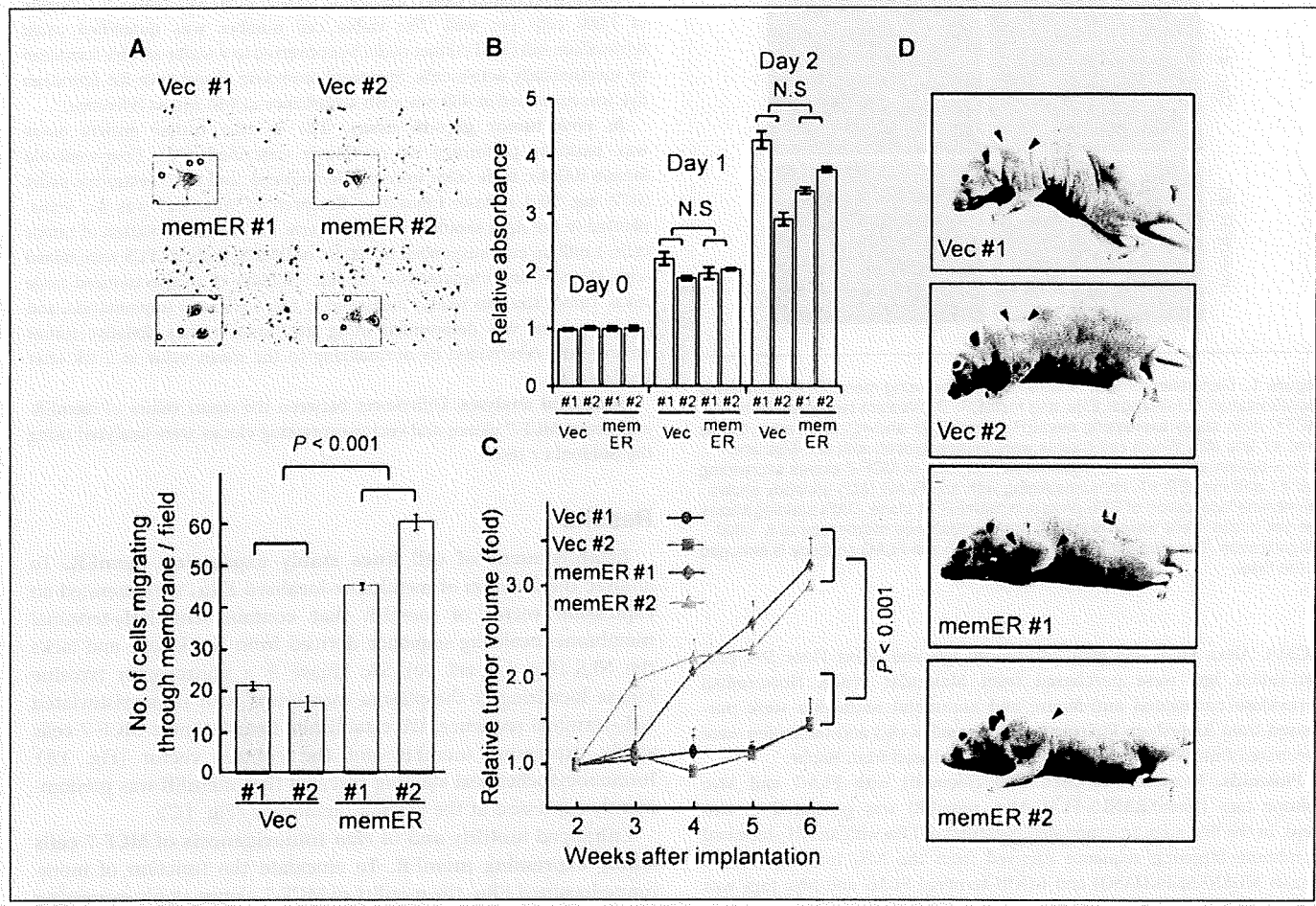

Figure 2. Enhanced motility and *in vivo* tumorigenesis of MCF-7 cells expressing memER. *A*, enhanced motility of memER-expressing MCF-7 cells. Number of cells migrating through a polyethylene terephthalate filter with 8-μm pores was counted for each clone. *Top*, cells on the lower side of the filters were stained with Giemsa's staining solution and visualized under a microscope. Representative views used to count the cells are shown at a ×200 magnification. Magnified views of membrane pores and migrating cells are shown in the insets. *Bottom, columns*, mean number of cells counted in five fields; *bars*, SE. *B*, MemER expression does not markedly affect *in vitro* cell proliferation. MCF-7 clones were seeded at a density of 1,000 cells per well and the cell growth was assayed using WST-8 tetrazolium salt. *Columns*, mean of relative absorbance at 450 nm for each clone normalized to values at day 0 ($n = 4$); *bars*, SE. *N.S.*, not significant. *C*, growth of xenograft derived from MCF-7 clones expressing memER is significantly accelerated compared with vector clones. Xenografts were established by s.c. implantation of MCF-7 clones in nude mice (one million cells per mouse). Tumor volume is shown by fold change normalized to the value at 2 wk after implantation. *Points*, mean of relative tumor volume (*vec #1*, $n = 4$; *vec #2*, $n = 3$; *memER #1*, $n = 4$; *memER #2*, $n = 7$); *bars*, SE. *D*, photographs of representative mice 8 wk after the implantation of MCF-7 clones. *Arrowhead*, tumor mass.

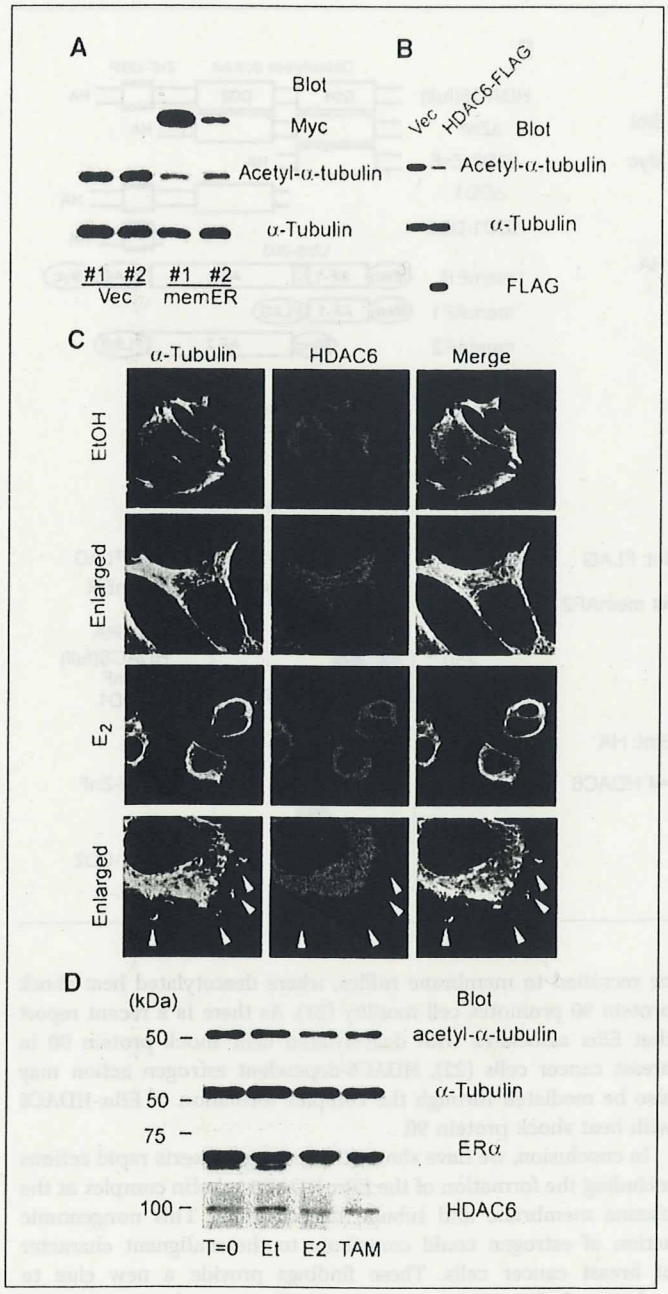

Figure 3. Estrogen reduces tubulin acetylation and translocates HDAC6 to the plasma membrane in MCF-7 cells. *A*, tubulin in memER-expressing MCF-7 clones is less acetylated. Whole cell lysates of indicated clones were immunoblotted with anti-Myc (*top*), anti–acetyl-α-tubulin (*middle*), and anti–α-tubulin (*bottom*). *B*, tubulin deacetylase activity of HDAC6. COS-7 cells were transiently transfected with empty or HDAC6-FLAG vectors. Cells were lysed at 24 h after transfection and immunoblotted with anti–acetyl-α-tubulin (*top*), anti–α-tubulin (*middle*), and anti-FLAG (M5; *bottom*). *C*, rapid translocation of HDAC6 to the plasma membrane in response to estrogen. MCF-7 cells were grown in an estrogen-starved medium for 48 h and treated with 17β-estradiol (E_2; 10 nmol/L) or vehicle (0.1% ethanol) for 15 min. Cells were immunostained with anti–α-tubulin (*green*) and anti-HDAC6 (*red*) and visualized with fluorescence microscopy at a ×600 magnification. Concentration of HDAC6 immunoreactivity at the plasma membrane is shown in E_2-stimulated cells. *Enlarged panels*, magnified views of a part of the top panels. Membrane protrusions (*white arrowheads*) are shown in enlarged panels of E_2-stimulated cells. *D*, rapid deacetylation of tubulin in MCF-7 cells with estrogen stimulation. MCF-7 cells were treated with E_2 (100 nmol/L), tamoxifen (*TAM*; 10 μmol/L), or vehicle (*Et*) for 15 min. Whole-cell lysates before (*T = 0*) and after drug treatment were immunoblotted with anti–acetyl-α-tubulin (*top*), anti–α-tubulin (*top middle*), anti-ERα (*bottom middle*), and HDAC6 (*bottom*). The acetylated level of tubulin is reduced in lysates from E_2- and tamoxifen-stimulated cells.

interact with the microtubule network and cause tubulin deacetylation.

Ligand-dependent association of HDAC6 with ERα. To prove the hypothesis that ERα associates with HDAC6 at the plasma membrane, memER and HA-tagged HDAC6 were cotransfected in 293T cells. An immunoprecipitation study verified the physical interaction of memER and HDAC6 proteins in an E_2-dependent manner. Tamoxifen also induced a weak interaction between memER and HDAC6 (Fig. 4*A*).

To analyze the responsible domains for the association of HDAC6 and memER, we generated a series of HA-tagged HDAC6 expression vectors with various functional domains deleted (Fig. 4*B*). HDAC6 includes two deacetylase domains (DD1 and DD2) and one ubiquitin carboxyl-terminal hydrolase-like zinc finger domain (ZnF-UBP). A transfection study revealed that these HDAC6 deletion mutants were expressed predominantly in the cytoplasm (data not shown). As ERα deletion mutants, we used memAF1 and memAF2 expression vectors, including the entire A/B region of ERα containing the AF-1 domain and the entire E/F region containing the activation function 2 domain, respectively, with an NH_2-terminal membrane–targeted sequence. We previously showed that these ERα deletion mutants were predominantly localized in the cytoplasm (6). The immunoprecipitation study revealed that the membrane-targeted activation function 2 domain associated with HDAC6 (Fig. 4*C*), and the DD2 domain of HDAC6 was responsible for the interaction with memER (Fig. 4*D*).

Discussion

Posttranslational modification is an important factor for the regulation of protein structure and function. Phosphorylation by protein kinases such as phosphatidylinositol-3-OH kinase and mitogen-activated protein kinase has been shown to play a critical role in estrogen-dependent nongenomic action. In the present study, we show that estrogen caused the formation of the ERα-HDAC6-tubulin complex at the plasma membrane and rapid tubulin deacetylation in MCF-7 breast cancer cells. Our findings show a novel aspect of estrogen nongenomic action that is regulated by tubulin acetylation, which is distinct from the previously reported mechanism dependent on protein phosphorylation.

In MCF-7 cells, estrogen-dependent tubulin deacetylation would be one of the driving forces of cell motility, as the microtubule network including tubulin is a critical element in cell migration. Our findings are consistent with a previous report that HDAC6 overexpression caused tubulin deacetylation and enhanced motility of breast cancer cells and the inhibition of HDAC6 activity reduced motility (9). HDAC6 inhibition is also considered to decrease turnover of focal adhesion, an interface between the cell membrane and the extracellular matrix. Decreased turnover of focal adhesion results in reduced cell motility (13).

It is also notable that memER accelerated tumor growth of MCF-7 cells in nude mice without enhancing cell proliferation *in vitro*. *In vivo* tumor growth differs from *in vitro* proliferation in the aspect that *in vivo* tumor growth requires several factors including anoikis resistance, angiogenesis, and survival in the hypoxic environment. Anoikis is a form of apoptosis caused by absence of attachment to the extracellular matrix (14). It was reported recently that HDAC6 is critical for anoikis resistance and *in vivo* tumorigenic growth with human ovarian cancer SKOV3 cells (15). In another report, stability of microtubules was shown to be associated with anoikis through alteration of the focal adhesion

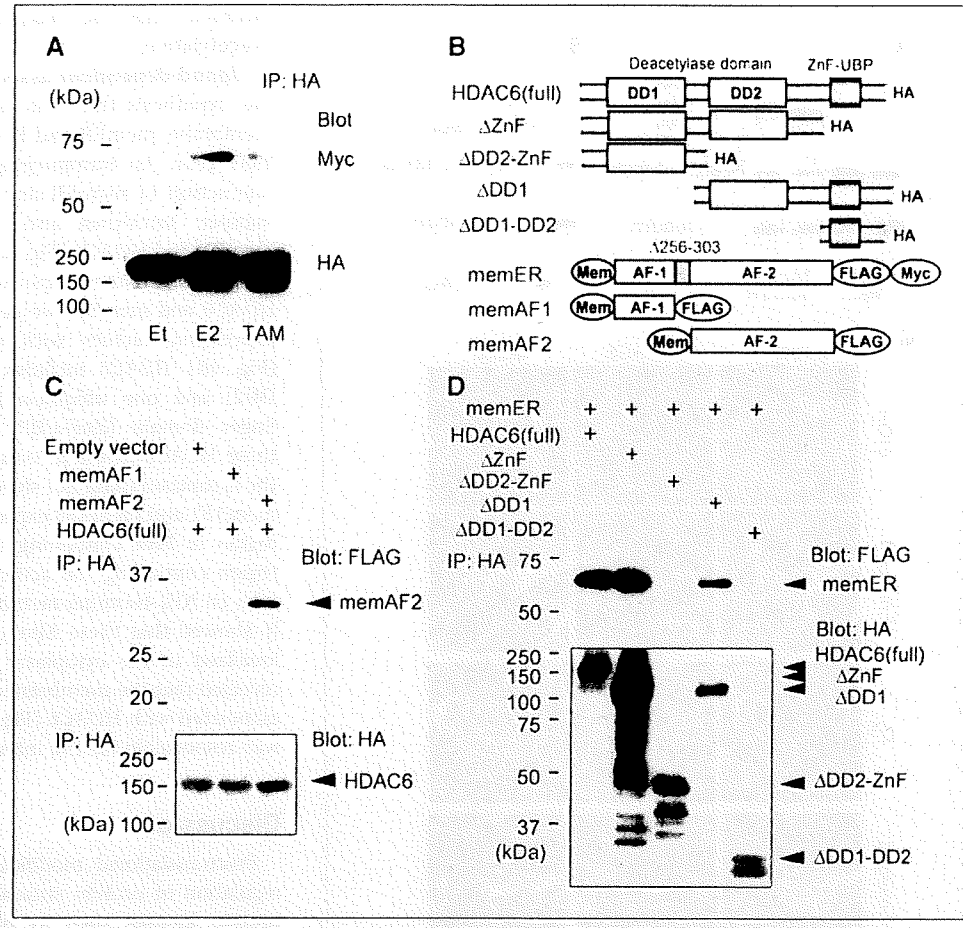

Figure 4. MemER associates with HDAC6. *A*, ligand-dependent association of memER and HDAC6. 293T cells were grown in estrogen-starved medium for 24 h and cotransfected with memER and HDAC6-FLAG. After 24-h incubation, cells were treated with E_2 (100 nmol/L), tamoxifen (10 μmol/L), and vehicle for 6 h. Whole cell lysates were immunoprecipitated with anti-HA. Immunoprecipitants by anti-Myc were subjected to immunoblotting with anti-Myc antibody (*top*) and anti-HA antibody (*bottom*). *B*, schematic representation of deletion mutants of HA-tagged HDAC6 and memER. *C*, ERα binds to HDAC6 through its activation function 2 domain. 293T cells were cotransfected with HDAC6-HA (full) and FLAG-tagged ERα deletion mutants. After 24-h incubation, cells were lysed and immunoprecipitated with anti-HA. Immunoprecipitants were immunoblotted with anti-FLAG (M5) antibody (*top*) and anti-HA antibody (*bottom*). *D*, HDAC6 binds to ERα with its deacetylase domain 2. 293T cells were cotransfected with memER and HA-tagged HDAC6 plasmids. After 24-h incubation, cells were lysed and immunoprecipitated with anti-HA. Immunoprecipitants were immunoblotted with anti-FLAG (M5) antibody (*top*) and anti-HA antibody (*bottom*).

structure (16). Although the direct effect of tubulin deacetylation is not evaluated in these reports, it is possible that deacetylated tubulin affects focal adhesion turnover and regulates anoikis resistance.

Because HDAC6 itself is reported as an estrogen-induced gene and HDAC6 overexpression is shown to enhance cell motility (8, 9), the estrogen-dependent up-regulation of HDAC6 could further potentiate its enzymatic activity. In this case, the genomic action of estrogen would promote its nongenomic action in MCF-7 cells. In contrast, the tamoxifen-induced nongenomic action would be unfavorable for the antagonistic function of this drug in the genomic action. We showed that tamoxifen also caused the interaction of memER with HDAC6 and tubulin deacetylation in MCF-7 cells. We assume that HDAC6-dependent tubulin deacetylation contributes to the increased cell motility and invasive migration of breast cancer cells; thus, this nongenomic action of the tamoxifen-induced tubulin deacetylation could be one of the reasons for tamoxifen resistance in breast cancer treatment. Indeed, several clinical trials have shown the superiority of aromatase inhibitors over tamoxifen in the first-line endocrine therapy for postmenopausal women with both early-stage and advanced breast cancers (17, 18). There is also a report that has shown tamoxifen-induced redistribution of ERα to the extranuclear region and the activation of nongenomic action via the epidermal growth factor receptor pathway (19), which would provide another mechanism for tamoxifen resistance.

HDAC6 also deacetylates another cytosolic protein, heat shock protein 90 (20). It has been shown that heat shock protein 90 could be recruited to membrane ruffles, where deacetylated heat shock protein 90 promotes cell motility (21). As there is a recent report that ERα associates with deacetylated heat shock protein 90 in breast cancer cells (22), HDAC6-dependent estrogen action may also be mediated through the complex formation of ERα-HDAC6 with heat shock protein 90.

In conclusion, we have shown that estrogen exerts rapid actions including the formation of the ERα-HDAC6-tubulin complex at the plasma membrane and tubulin deacetylation. This nongenomic action of estrogen could contribute to the malignant character of breast cancer cells. These findings provide a new clue to understand the mechanisms underlying the pathophysiology of breast cancer and the resistance to endocrine therapy, and to develop new molecular targets for breast cancer treatment.

Disclosure of Potential Conflicts of Interest

No potential conflicts of interest were disclosed.

Acknowledgments

Received 9/9/08; revised 1/6/09; accepted 1/9/09; published OnlineFirst 3/24/09.

Grant support: Genome Network Project and DECODE from the Ministry of Education, Culture, Sports, Science and Technology, Grants from the Japan Society for the Promotion of Science, and Grants-in-Aid from the Ministry of Health, Labor and Welfare.

The costs of publication of this article were defrayed in part by the payment of page charges. This article must therefore be hereby marked *advertisement* in accordance with 18 U.S.C. Section 1734 solely to indicate this fact.

We thank Dr. Stuart L. Schreiber for providing HDAC6 cDNA and A. Okada for his technical assistance.

References

1. Rabaglio M, Aebi S, Castiglione-Gertsch M. Controversies of adjuvant endocrine treatment for breast cancer and recommendations of the 2007 St Gallen conference. Lancet Oncol 2007;8:940–9.
2. Cheskis BJ, Greger JG, Nagpal S, Freedman LP. Signaling by estrogens. J Cell Physiol 2007;213:610–7.
3. Simoncini T, Hafezi-Moghadam A, Brazil DP, et al. Interaction of oestrogen receptor with the regulatory subunit of phosphatidylinositol-3-OH kinase. Nature 2000;407:538–41.
4. Kousteni S, Bellido T, Plotkin LI, et al. Nongenotropic, sex-nonspecific signaling through the estrogen or androgen receptors: dissociation from transcriptional activity. Cell 2001;104:719–30.
5. Migliaccio A, Di Domenico M, Castoria G, et al. Tyrosine kinase/p21ras/MAP-kinase pathway activation by estradiol-receptor complex in MCF-7 cells. EMBO J 1996;15:1292–300.
6. Azuma K, Horie K, Inoue S, Ouchi Y, Sakai R. Analysis of estrogen receptor α signaling complex at the plasma membrane. FEBS Lett 2004;577:339–44.
7. Hubbert C, Guardiola A, Shao R, et al. HDAC6 is a microtubule-associated deacetylase. Nature 2002;417:455–8.
8. Yoshida N, Omoto Y, Inoue A, et al. Prediction of prognosis of estrogen receptor-positive breast cancer with combination of selected estrogen-regulated genes. Cancer Sci 2004;95:496–502.
9. Saji S, Kawakami M, Hayashi S, et al. Significance of HDAC6 regulation via estrogen signaling for cell motility and prognosis in estrogen receptor-positive breast cancer. Oncogene 2005;24:4531–9.
10. Rai D, Frolova A, Frasor J, Carpenter AE, Katzenellenbogen BS. Distinctive actions of membrane-targeted versus nuclear localized estrogen receptors in breast cancer cells. Mol Endocrinol 2005;19:1606–17.
11. Azuma K, Tanaka M, Uekita T, et al. Tyrosine phosphorylation of paxillin affects the metastatic potential of human osteosarcoma. Oncogene 2005;24:4754–64.
12. Urano T, Saito T, Tsukui T, et al. Efp targets 14-3-3 σ for proteolysis and promotes breast tumour growth. Nature 2002;417:871–5.
13. Tran AD, Marmo TP, Salam AA, et al. HDAC6 deacetylation of tubulin modulates dynamics of cellular adhesions. J Cell Sci 2007;120:1469–79.
14. Reddig PJ, Juliano RL. Clingling to life: cell to matrix adhesion and cell survival. Cancer Metastasis Rev 2005;24:425–39.
15. Lee YS, Lim KH, Guo X, et al. The cytoplasmic deacetylase HDAC6 is required for efficient oncogenic tumorigenesis. Cancer Res 2008;68:7561–9.
16. Deschesnes RG, Patenaude A, Rousseau JL, et al. Microtuble-destabilizing agents induce focal adhesion structure disorganization and anoikis in cancer cells. J Pharmacol Exp Ther 2007;320:853–64.
17. Thurlimann B, Keshaviah A, Coates AS, et al. A comparison of letrozole and tamoxifen in postmenopausal women with early breast cancer. N Engl J Med 2005;353:2747–57.
18. Mouridsen H, Gershanovich M, Sun Y, et al. Phase III study of letrozole versus tamoxifen as first-line therapy of advanced breast cancer in postmenopausal women: analysis of survival and update of efficacy from the International Letrozole Breast Cancer Group. J Clin Oncol 2003;21:2101–9.
19. Fan P, Wang J, Santen RJ, Yue W Long-term treatment with tamoxifen facilitates translocation of estrogen receptor α out of the nucleus and enhances its interaction with EGFR in MCF-7 breast cancer cells. Cancer Res 2007;67:1352–60.
20. Kovacs JJ, Murphy PJ, Gaillard S, et al. HDAC6 regulates Hsp90 acetylation and chaperone-dependent activation of glucocorticoid receptor. Mol Cell 2005;18:601–7.
21. Gao YS, Hubbert CC, Lu J, et al. Histone deacetylase 6 regulates growth factor-induced actin remodeling and endocytosis. Mol Cell Biol 2007;27:8637–47.
22. Fiskus W, Ren Y, Mohapatra A, et al. Hydroxamic acid analogue histone deacetylase inhibitors attenuate estrogen receptor-α levels and transcriptional activity: a result of hyperacetylation and inhibition of chaperone function of heat shock protein 90. Clin Cancer Res 2007;13:4882–90.

Expression of CUB domain containing protein (CDCP1) is correlated with prognosis and survival of patients with adenocarcinoma of lung

Jun-ichiro Ikeda,[1] Tomofumi Oda,[1,2] Masayoshi Inoue,[2] Takamasa Uekita,[3] Ryuichi Sakai,[3] Meinoshin Okumura,[2] Katsuyuki Aozasa[1] and Eiichi Morii[1,4]

Departments of [1]Pathology and [2]Thoracic Surgery, Osaka University Graduate School of Medicine, 2-2 Yamada-oka, Suita, Osaka, and [3]Growth Factor Division, National Cancer Center Research Institute, 5-1-1 Tsukiji, Chuo-ku, Tokyo, Japan

(Received September 29, 2008/Revised November 4, 2008/Accepted November 19, 2008/Online publication December 11, 2008)

CUB domain containing protein (CDCP1), a transmembrane protein with intracellular tyrosine residues which are phosphorylated upon activation, is supposed to be engaged in proliferative activities and resistance to apoptosis of cancer cells. Expression level of CDCP1 was examined in lung adenocarcinoma, and its clinical implications were evaluated. CDCP1 expression was immunohistochemically examined in lung adenocarcinoma from 200 patients. Staining intensity of cancer cells was categorized as low and high in cases with tumor cells showing no or weak and strong membrane staining, respectively. MIB-1 labeling index was also examined. There were 113 males and 87 females with median age of 63 years. Stage of disease was stage I in 144 cases (72.0%), II in 19 (9.5%), and III in 37 (18.5%). Sixty of 200 cases (30.0%) were categorized as CDCP1-high, and the remaining as CDCP1-low. Significant positive correlation was observed between CDCP1-high expression and relapse rate ($P < 0.0001$), poor prognosis ($P < 0.0001$), MIB-1 labeling index ($P < 0.0001$), and occurrence of lymph node metastasis ($P = 0.0086$). There was a statistically significant difference in disease-free survival (DFS) ($P < 0.0001$) and overall survival (OS) rates ($P < 0.0001$) between patients with CDCP1-high and CDCP1-low tumors. Univariate analysis showed that lymph node status, tumor stage, and CDCP1 expression were significant factors for both OS and DFS. Multivariate analysis revealed that only CDCP1 expression was an independent prognostic factor for both OS and DFS. CDCP1 expression level is a useful marker for prediction of patients with lung adenocarcinoma (*Cancer Sci* 2009; 100: 429–433).

Introduction

Since 1985 lung cancer has been the most common cause of cancer death in the world.[1] Non-small cell lung cancer (NSCLC) comprises 75–85% of all lung cancers, and approximately two-thirds of NSCLC patients have advanced stages at diagnosis. Despite the advances in the methods for detection and treatment of lung cancer, prognosis of NSCLC patients still remains unfavorable. Therefore, it is important to clarify the mechanism of tumor biology, and establishment of effective therapeutic modalities is essential to improve the prognosis in NSCLC. Previous studies accumulated information regarding the factors influencing prognosis in NSCLC. They include clinical, pathological, and molecular factors.

CUB domain containing protein (CDCP1) was originally identified as an epithelial tumor antigen by comparisons of molecules expressed in lung cancer cell lines and normal lung tissues.[2] CDCP1 is a transmembrane protein with three extracellular CUB domains, which are important for cell–cell interactions, and intracellular tyrosine residues which are phosphorylated upon activation.[2–7] Previously, we reported the epigenetic regulation of CDCP1 expression in the cell lines derived from various malignancies and clinical samples of breast cancer.[8,9] The CDCP1 expression level correlated with proliferative activities of breast cancer cells in the clinical samples.[8] Very recently, CDCP1 was reported to protect cells from anoikis, a form of apoptosis triggered by the loss of cell survival signals generated from interaction of cells with the extracellular matrix.[10] The knocked-down expression of CDCP1 by RNA interference abolished in vitro colony formation and in vivo metastatic abilities of lung adenocarcinoma cell line A549.[10] These findings showed that CDCP1 is required for protection of cells from anoikis, and suggest an important role of CDCP1 for tumorigenesis and metastasis, at least in cell lines. In the present study, CDCP1 expression was immunohistochemically examined in clinical samples from lung adenocarcinoma, and its clinical implications were evaluated.

Materials and Methods

Patients and tissue samples. Two hundred patients who underwent surgery for lung adenocarcinoma at Osaka University Hospital during the period from January 1993 to January 2004 were examined. Clinicopathological findings in these 200 patients are summarized in Table 1. There were 113 men and 87 women with ages ranging from 33 to 82 years (median, 63). Resected specimens were macroscopically examined to determine the location and size of the tumors. The size of the main tumor ranged from 8 to 70 mm (median, 24.5). The histological stage was determined according to the 6th edition of the Union International Contre le Cancer – TNM staging system.[11] Histologic specimens were fixed in 10% formalin and routinely processed for paraffin-embedding. Paraffin-embedded specimens were stored in the dark room in the Department of Pathology of Osaka University Hospital at room temperature, and were sectioned at 4-μm thickness at the time of staining. In some cases, total RNA was extracted using RNeasy kit (Qiagen, Valencia, CA, USA) with DNase I treatment. All patients were followed up with laboratory examinations including routine peripheral blood cell counts at 1- to 6-month intervals, chest roentgenogram, computed tomographic scan of the chest, and endoscopic examinations of the bronchus at 6- to 12-month intervals. The follow-up period for survivors ranged from 5 to154 months (median, 63). The study was approved by the ethical review board of the Graduate

This work is original, and contains no materials previously presented in any reports and publications.

[4]To whom correspondence should be addressed.
E-mail: morii@patho.med.osaka-u.ac.jp

doi: 10.1111/j.1349-7006.2008.01066.x

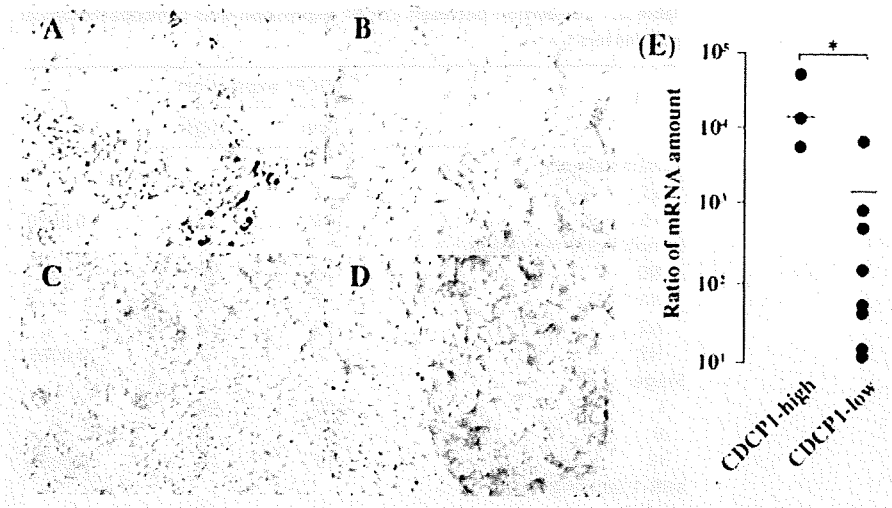

Fig. 1. Surface staining of CDCP1-low (A and B) and -high (C and D) cases, ×400 (E) Real-time reverse transcription–polymerase chain reaction. The amount of CDCP1 mRNA was significantly higher in immunohistochemically defined CDCP1-high cases than in CDCP1-low cases. The bar shows mean values of the amount of CDCP1 mRNA. *$P < 0.01$

Table 1. Summary of characteristics in 200 pulmonary adenocarcinoma patients

Sex	Number of patients
Male	113
Female	87
Tumor size (cm)	
≥5	12
<5	187
Lymph node metastasis	
N0	159
N1	8
N2	29
N3	4
Stage	
I	144
II	19
III	37
Recurrence	
Positive	60
Negative	140
Prognosis	
Dead	41
Alive (with recurrence)	24
Alive (with no recurrence)	135

School of Medicine, Osaka University. Informed consent was obtained from each patient.

Immunohistochemistry for CDCP1, phosphorylated CDCP1 and Ki-67. CDCP1 expression was immunohistochemically examined with use of anti-CDCP1 (Abcam Ltd, Cambridge, UK) and antiphosphorylated CDCP1 antibody. The antiphosphorylated CDCP1 antibody recognizes CDCP1 phosphorylated at Tyr734 and can be used for immunostaining on paraffin-embedded sections.[10,12] The proliferative activity of cancer cells was examined with monoclonal antibody MIB-1 (Immunotech, Marseilles, France), recognizing the proliferation-associated antigen Ki-67. After antigen retrieval with Pascal pressurized heating chamber (Dako, Glostrup, Denmark), the sections were incubated with anti-CDCP1, phosphorylated CDCP1 antibody and MIB-1, diluted at ×200, ×400 and ×100, respectively. Then, the sections were treated with biotin-conjugated antigoat IgG (Zymed, San Francisco, CA, USA) for CDCP1 staining, or with biotin-conjugated antimouse IgG (Dako) for phosphorylated CDCP1 and MIB-1 staining. After washing, the sections were incubated with the peroxidase-conjugated biotin-avidin complex (Vectastain ABC kit, Vector Laboratories, Burlingame, CA, USA). diaminobenzidine (Vector Laboratories) was used as a chromogen. As the negative control, staining was carried out in the absence of a primary antibody. Stained sections were evaluated independently by two pathologists (JI and EM). Generally, CDCP1 expression levels varied among tumor cells in the same case. Staining intensity of tumor cells was divided into four categories; tumor cells with no (representative field was demonstrated in Fig. 1A), weak (Fig. 1B), moderate (Fig. 1C), or strong (Fig. 1D) membrane staining. The intensity of CDCP1 expression in each case was defined by the major population of staining as follows: cases with tumor cells showing no or weak membrane staining were categorized as CDCP1-low, and those showing moderate or strong membrane staining as CDCP1-high. The MIB-1 labeling index was defined as the percentage of stained nuclei per 1000 cells. The cases were divided into MIB-1-high and MIB-1-low groups using the median as cut-off value.

Quantification of mRNA by real-time reverse transcription-polymerase chain reaction (RT-PCR). To evaluate the specificity of CDCP1 immunostaining, expression level of CDCP1 at mRNA and protein levels was compared. For this, fresh frozen materials were available in 13 of the 200 cases. Total RNA was extracted using RNeasy kit (Qiagen, Valencia, CA, USA) with DNase I treatment. Two micrograms of total RNA was subjected to reverse transcription using Superscript III (Invitrogen, Carlsbad, CA, USA). The mRNA levels for CDCP1 and glyceraldehyde-3-phosphate dehydrogenase (GAPDH) genes were verified using TaqMan Gene Expression Assays (Hs00224587_m1 and 4310884E, respectively; Applied Biosystems, Foster City, CA, USA) as recommended by the manufacturer. The amount of CDCP1 mRNA was normalized to that of GAPDH mRNA.

Statistical analysis. Statistical analyses were performed using StatView software (SAS Institute Inc., Cary, NC, USA). The Chi-square and Fisher's exact probability test were used to analyze the correlation between CDCP1 expression and clinicopathological factors in pulmonary adenocarcinoma. Kaplan-Meier methods were used to calculate overall survival (OS) and disease-free survival (DFS) rate, and differences in survival curves were evaluated with the log-rank test. Cox's proportional hazards regression model with a stepwise manner was used to analyze the independent prognostic factors. The P-values of less than 0.05 were considered to be statistically significant.

Results

Tumor stages in the present patients were: stage I in 144 patients (72.0%); II in 19 patients (9.5%); and III in 37 patients (18.5%). The histological types of tumors were: bronchioloalveolar

doi: 10.1111/j.1349-7006.2008.01066.x

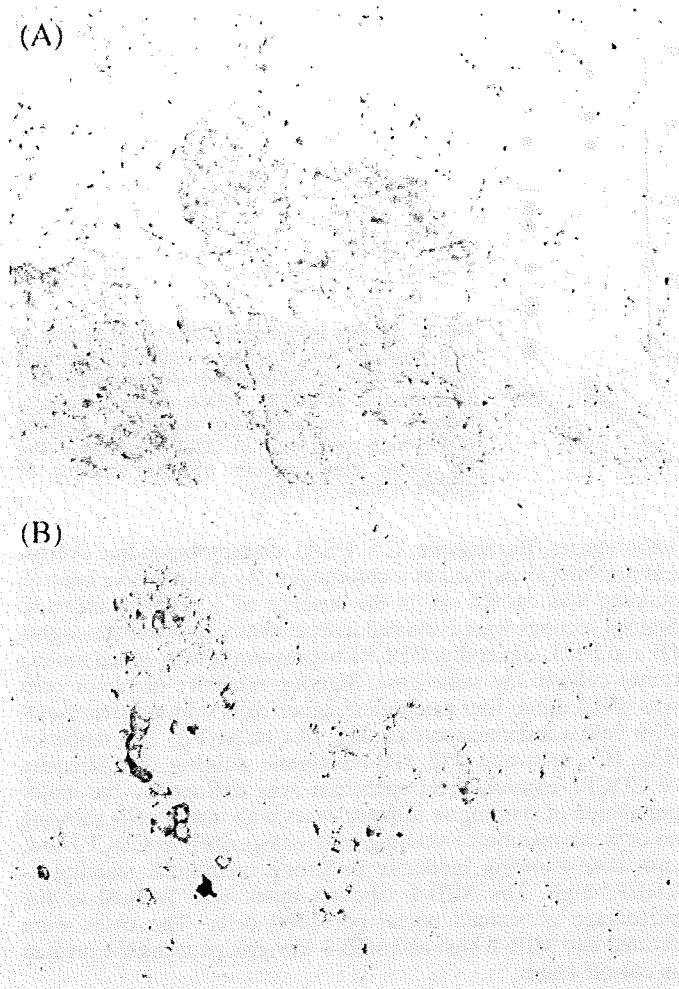

Fig. 2. Localization of phosphorylated CDCP1 in lung adenocarcinoma. Stained cells with anti-CDCP1 antibody (A), and antiphosphorylated CDCP1 antibody (B). Among the CDCP1-positive tumor cells, peripheral areas of tumor cell nests were stained with antiphophorylated CDCP1 antibody, × 400.

(62 patients, 31.0%); papillary (48 patients, 24.0%); or mixed bronchioloalveolar and papillary adenocarcinoma (90 patients, 45.0%). The 5-year DFS and OS was 78.7% and 80.6%, respectively. Tumors recurred in 60 patients. Of these, 38 patients died due to the tumors.

To evaluate the specificity of immunohistochemical staining for CDCP1 expression, quantitative real-time RT-PCR was performed: expression levels of CDCP1 at protein and mRNA level was compared in 13 cases (3 CDCP1-high and 10 CDCP1-low cases at immnohistochemical results). The amount of CDCP1 mRNA was significantly higher in cases with CDCP1-high expression at immunohistochemistry than those with CDCP1-low expression ($P < 0.01$, Fig. 1E). These results showed that the immunohistochemical evaluation is a reliable method for evaluation of CDCP1 expression.

Immunohistochemical detection of CDCP1 expression was carried out in 200 lung adenocarcinoma tissues. Sixty of 200 cases (30.0%) were categorized as CDCP1-high, and the remaining as CDCP1-low. Representative staining results were illustrated in Fig. 1(A–D).

Intracellular tyrosine residues of CDCP1 are known to be phosphorylated upon activation in vitro. To examine the localization of activated CDCP1, 43 cases of CDCP1-high lung adenocarcinoma tissues were stained with antiphosphorylated CDCP1. Phosphorylated CDCP1 was detected only in a small portion of CDCP1-expressing cells (Fig. 2 A and 2B), which

Table 2. Correlation between CDCP1 expression and clinicopathological parameters

	CDCP1 expression		*P*
	Low	High	
Tumor size (cm)			
≥5	7	5	
<5	133	55	0.3630
Lymph node metastasis			
N0	120	39	
N1	3	5	
N2	15	14	
N3	2	2	0.0086
Stage			
I	110	34	
II	11	8	
III	19	18	0.0059
MIB-1 labeling index			
≥5%	56	45	
<5%	84	15	<0.0001
Recurrence			
Positive	23	37	
Negative	117	23	<0.0001
Prognosis			
Dead	17	24	
Alive (with recurrence)	10	14	
Alive (with no recurrence)	113	22	<0.0001

appeared to be localized to the peripheral areas of tumor cell nests. Cells without CDCP1 expression did not show any phosphorylated CDCP1 signals, indicating the specificity of the antiphophorylated CDCP1 antibody. Phosphorylated CDCP1 was detected in 19 out of 43 cases: any significant clinicopathological differences were not observed between cases with and without phosphorylated CDCP1.

Correlation of CDCP1 expression with the clinicopathological features was evaluated. Significant positive correlation was observed between CDCP1-high expression and relapse rate ($P < 0.0001$), poor prognosis ($P < 0.0001$), MIB-1 labeling index ($P < 0.0001$), and occurrence of lymph node metastasis ($P = 0.0086$). Other parameters including tumor size and stage did not correlate with CDCP1 expression (Table 2). There was a statistically significant difference in DFS rates ($P < 0.0001$) and OS rates ($P < 0.0001$) between patients with CDCP1-high and CDCP1-low tumors (Fig. 3).

Univariate analysis showed that lymph node status, tumor stage, and CDCP1 expression were significant factors for both OS and DFS (Table 3). The multivariate analysis revealed that only CDCP1 expression was an independent prognostic factor for both OS and DFS.

Discussion

Patient characteristics such as the gender (male preponderance), age distribution (median age, 6th decades of life), and 5-year OS of approximately 80% in the present study were similar to those in a previous report on the lung adenocarcinoma.[13] In addition, the univariate analysis showed the prognostic significance of occurrence of lymph node metastasis and stage of disease, as reported previously.[13] These findings indicate that the results obtained from the present cases are commonly applicable.

Among the clinicopathological factors examined, high CDCP1 expression level correlated with increased occurrence of lymph node metastasis and tumor relapse. A previous study using the lung adenocarcinoma cell lines indicated a significant role of CDCP1 for anchorage-independent growth of tumor cells.[10]

Table 3. Univariate and multivariate analyses of prognostic factors for overall and disease-free survivals

	Overall survival				Disease-free survival			
	Univariate		Multivariate		Univariate		Multivariate	
	HR (95% CI)	*P*-value	HR (95% CI)	*P*-value	HR (95% CI)	*P*-value	HR (95% CI)	*P*-value
Tumor size	1.07 (0.79–1.43)	0.672			1.11 (0.86–1.45)	0.425		
Lymph node status	2.34 (1.77–3.08)	<0.001	1.46 (0.85–2.50)	0.167	2.40 (1.82–3.17)	<0.001	1.43 (0.84–2.40)	0.182
Stage	2.64 (1.90–3.69)	<0.001	1.63 (0.87–3.06)	0.128	2.77 (1.99–3.86)	<0.001	1.74 (0.95–3.20)	0.074
MIB-1 labeling index	1.46 (0.78–2.74)	0.235			1.44 (0.77–2.69)	0.250		
CDCP1 expression	4.11 (2.18–7.75)	<0.001	2.89 (1.51–5.54)	0.001	4.32 (2.31–8.08)	<0.001	3.04 (1.60–5.80)	<0.001

HR, hazard ratio; CI, confidence interval.

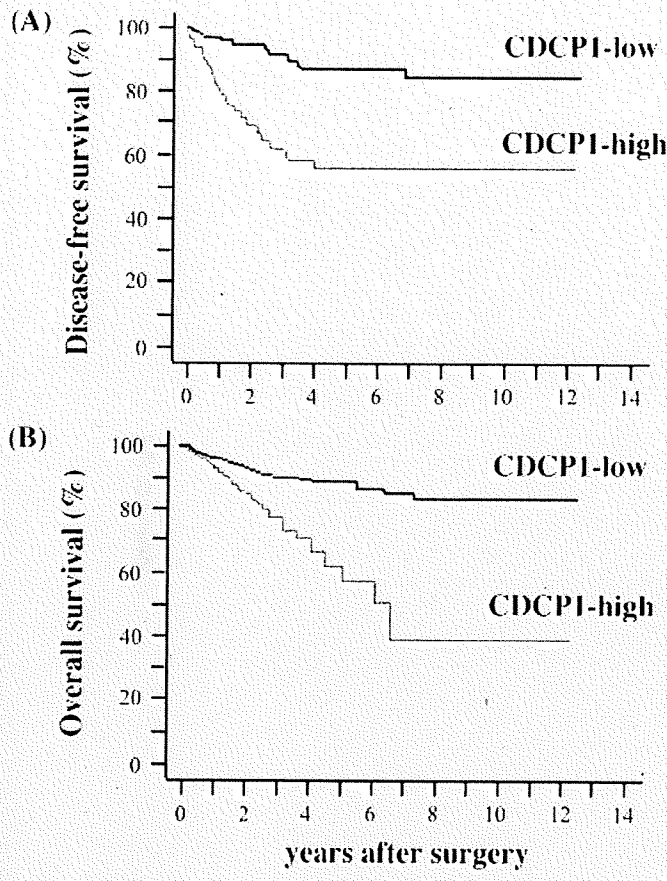

Fig. 3. Kaplan-Meier plots of disease-free (A) and overall survival (B) of patients.

The knocked-down expression of CDCP1 abolished ability of in vitro colony formation in the A549 lung adenocarcinoma cell line.[10] In addition, when injected into nude mice, the number of metastatic nodules was low in CDCP1-knocked down A549 cells as compared to parental A549 cells.[10] Taken together with the present results, CDCP1 appeared to play important roles for metastatic and tumorigenic potentials of lung adenocarcinoma not only in cell lines but also in clinical samples.

High CDCP1 expression was correlated with MIB-1 labeling index. Since the monoclonal antibody MIB-1 recognizes Ki-67 antigen that is expressed in cells during the cell cycle, except at the G0 phase, it can be applied to evaluate the proliferative activities of cells. Previously, we showed the positive correlation of CDCP1 expression with MIB-1 labeling index in breast cancer cells.[8] These findings indicate that CDCP1 expression level reflects a proliferative activity of cancer cells.

Intracellular tyrosine residues of CDCP1 are known to be phosphorylated upon activation, and the level of tyrosine phosphorylation is associated with the capacity for anchorage independence in A549 cells.[10] Immunohistochemically, phosphorylated CDCP1 was found to be localized to the peripheral areas of tumor cell nests. Lung adenocarcinoma cells often show bronchioalveolar growth in the periphery of the cancer tissues, but such portions were almost negative for phosphorylated CDCP1 expression. Phosphorylated CDCP1 was mostly present in the tumor cells expanding to the surrounding normal tissues. This was consistent with the previous report that phosphorylated CDCP1 is localized in the invasive front of gastric cancer.[12] Therefore, phosphorylated CDCP1 may play some roles for tumor invasion, in addition to anchorage independence. The staining for phosphorylated and non-phosphorylated CDCP1 demonstrated that most tumor cells expressed CDCP1 as a non-phosphorylated form. This was consistent with the report by Brown et al. that the phosphorylation of CDCP1 is dynamically balanced by Src-family kinase and phosphotyrosine phosphatase activities, yielding low equilibrium phosphorylation.[6] CDCP1 contains three extracellular CUB domains, which might be involved in cell adhesion or interaction with the extracellular matrix.[2–7] Non-phosphorylated CDCP1 may function as an adhesion molecule.

Multivariate analysis revealed the high expression of CDCP1 to be an independent factor for poor prognosis for patients with lung adenocarcinoma. Benes et al. reported that Src, which mediates proliferation signals in cancers, forms a complex with phosphorylated CDCP1.[7] These findings indicate that overexpression of CDCP1 could stimulate tumor growth, explaining why prognosis of patients with CDCP1-high tumors is worse than that with CDCP1-low tumors.

In conclusion, high CDCP1 expression is an independent factor for poor prognosis of patients with lung adenocarcinoma. Further studies will be necessary to elucidate whether CDCP1 expression could be a useful marker for prediction of prognosis in other types of cancers. CDCP1 could be a molecular target for cancer therapy.

Acknowledgments

The authors thank Ms. Megumi Sugano and Ms. Takako Sawamura for their technical assistance. This work was supported by grants from the Ministry of Education, Culture, Sports, Science and Technology, and from the Osaka Cancer Research Foundation

doi: 10.1111/j.1349-7006.2008.01066.x

References

1 Parkin DM, Bray F, Ferlay J, Pisani P. Global Cancer Statistics, 2002. CA Cancer J Clin 2005; 55: 74–108.
2 Scherl-Mostageer M, Sommergruber W, Abseher R, Hauptmann R, Ambros P, Shweifer N. Identification of a novel gene, CDCP1, overexpressed in human colorectal cancer. Oncogene 2001; 20: 4402–8.
3 Hooper JD, Zijlstra A, Aimes RT et al. Subtractive immunization using highly metastatic human tumor cells identifies SIMA135/CDCP1, a 135 kDa cell surface phosphorylated glycoprotein antigen. Oncogene 2003; 22: 1783–94.
4 Conze T, Lammers R, Kuci S et al. CDCP1 is a novel marker for hematopoietic stem cells. Ann NY Acad Sci 2003; 996: 222–6.
5 Buhring H-J, Kuci S, Conze T et al. CDCP1 identifies a broad spectrum of normal and malignant stem/progenitor cell subsets of hematopoietic and nonhematopoietic origin. Stem Cells 2004; 22: 334–43.
6 Brown TA, Yang TM, Zaitsevskaia T et al. Adhesion or plasmin regulates tyrosine phosphorylation of a novel membrane glycoprotein p80/gp140/CUB domain-containing protein 1 in epithelia. J Biol Chem 2004; 279: 14772–83.
7 Benes CH, Wu N, Elia AEH, Dharia T, Cantley LC, Soltoff SP. The C2 domain of PKC-delta is a phosphotyrosine binding domain. Cell 2005; 121: 271–80.
8 Ikeda JI, Morii E, Kimura H et al. Epigenetic regulation of the expression of the novel stem cell marker CDCP1 in cancer cells. J Pathol 2006; 210: 75–84.
9 Kimura H, Morii E, Ikeda JI et al. Role of DNA methylation for expression of novel stem cell marker CDCP1 in hematopoietic cells. Leukemia 2006; 20: 1551–6.
10 Uekita T, Jia L, Narisawa-Saito M, Yokota J, Kiyono T, Sakai R. CUB domain-containing protein 1 is a novel regulator of anoikis resistance in lung adenocarcinoma. Mol Cell Biol 2007; 27: 7649–60.
11 Sobin LH, Wittekind Ch, eds. TNM Classification of Malignant Tumors, 5th edn. New York: John Wiley & Sons, Inc., 1997.
12 Uekita T, Tanaka M, Takigahira M et al. CUB domain-containing protein 1 regulates peritoneal dissemination of gastric scirrhous carcinoma. Am J Patho 2008; 172: 1729–39.
13 Suzuki K, Nagai K, Yoshida J et al. Conventional Clinicopathologic Prognostic Factors in Surgically Resected Nonsmall Cell Lung Carcinoma. Cancer 1999; 86: 1976–84.